

Autophagy and Spinal Muscular Atrophy: Towards a Pathway-Centric Therapy for a Fatal Childhood Disorder

Michael Hodgson

Dr Maria Dimitriadi, Dr Pryank Patel, Dr Simon Baines

Submitted to the University of Hertfordshire in partial fulfilment of the requirements of the degree of MSc by Research

November 2018

Abstract

Spinal muscular atrophy (SMA) is a devastating neuromuscular and the primary cause of infant death. SMA is characterised by the loss of motor neurons in the spinal resulting in progressive muscle atrophy, paralysis and respiratory defects leading to early childhood death. SMA is caused by a depletion of the ubiquitously expressed survival motor neuron (SMN) protein that performs a key regulatory function in the assembly of the eukaryotic mRNA splicing machinery and is thus required for the survival of all tissues. The genetic elements responsible for SMA are very well characterised but, after decades of research, it is still unknown why depletion of this ubiquitous specifically affects motor neurons. Numerous studies are now emerging that implicate disruption of autophagy, a highly conserved lysosomal degradative pathway responsible for the bulk removal of cytosolic cargo too large for the proteasome, in the disease pathology of SMA. In the present study, we utilise the powerful genetic tools of a *Caenorhabditis elegans* SMA model to delineate how disruptions in the autophagic pathway may contribute to SMA pathogenesis. Using an RNA interference genetic screen, we identified three putative modifiers of SMN loss of function neuromuscular defects in the *C. elegans* SMA model – *epg-8*, *sqst-1* and *atg-16.1*. In line with pre-existing studies, our results indicate that autophagy is disrupted in SMA, and that this disruption is likely occur during the initial regulatory stages of the pathway. Although further study will be required to identify the precise mechanisms through which this autophagic disruption occurs, these findings show that autophagy has promising potential for novel therapeutic targets.

Acknowledgements

First and foremost, I would like to extend my thanks to my principal supervisors Dr Maria Dimitriadi and Dr Pryank Patel for their endless support, guidance and patience throughout this project. Their support made the entire project possible and has helped transition into a better researcher.

I would also like to thank my fellow colleagues and Dimitriadi lab members for their general assistance and encouragement when I was feeling stressed and overwhelmed.

I would also like to extend my thanks Dr Diana Francis and the rest of the laboratory technical staff for their endless advice and assistance during the project period.

Finally, I would like to acknowledge University of Hertfordshire for allowing me access to their facilities which enabled me to complete this work.

Contents

Abstract	2
Acknowledgements	3
Contents	4
1 Introduction	6
1.1 – Spinal Muscular Atrophy.....	6
1.2 – Molecular Genetics of SMA	7
1.3 – The SMN Protein.....	9
1.4 – Genetic Modifiers of SMA	13
1.5 – SMA Therapeutic Strategies.....	15
1.6 – The Role of Autophagy in SMA	16
1.7 – <i>Caenorhabditis elegans</i> as a Model to Study SMA	23
1.8 – Project Aims & Objectives	24
2 Materials and Methods	25
2.1 – <i>Caenorhabditis elegans</i> strains and maintenance.....	25
2.2 – RNA interference by bacterial feeding	25
2.3 – Construction of RNA interference feeding clones for <i>atg-3</i> and <i>atg-4.2</i>	26
2.4 – RNA interference based genetic screen of <i>C. elegans</i> autophagy orthologs.....	27
2.5 – Pharyngeal pumping neuromuscular behavioural assay	27
2.6 – Data analysis	27
3 Results	28
3.1 – Neuromuscular Behavioural Assay	28
3.1.1 – <i>smn-1(ok355)</i> mutants exhibit pharyngeal pumping defects.....	28
3.2 – Generation of RNAi Feeding Clones	29
3.2.1 – Construction of <i>atg-3</i> and <i>atg-4.2</i> RNAi feeding constructs	29
3.3 – Genetic Screen of Autophagy Orthologs in the <i>C. elegans</i> SMA Model	31
3.3.1 – RNAi mediated knockdown of several autophagy genes likely have no effect on SMN loss of function neuromuscular defects.....	31
3.3.2 – Genetic screen identifies <i>epg-8</i> , <i>sqst-1</i> and <i>atg16.1</i> as putative modifiers of SMN loss of function neuromuscular defects.....	39
4 Discussion.....	43
4.1 – Main Findings.....	43
4.2 – Autophagy is Disrupted in SMA.....	44

4.3 – Genes Identified as Modifiers of SMN Loss of Function Defects.....	45
4.4 – Future Work.....	46
4.5 – Conclusions.....	47
5 References	48

1 Introduction

1.1 – Spinal Muscular Atrophy

Spinal muscular atrophy (SMA) is a devastating autosomal recessive neuromuscular disorder and the leading genetic cause of infant mortality, with an incidence rate of 1 in 6,000-10,000 live births and a carrier frequency of 1 in 40-50 adults (Verhaart et al., 2017). SMA is characterised by progressive muscle atrophy, paralysis and respiratory complications ultimately being the primary cause of childhood death (Monani & De Vivo, 2014). This muscle wastage occurs due to the gradual loss of α -motor neurons from the anterior horn of the spinal cord (D'Amico, Mercuri, Tiziano & Bertini, 2011), leading to a depletion in the levels of the ubiquitously expressed Survival Motor Neuron (SMN) protein. SMN is widely expressed in the nucleus and cytoplasm (Kolb & Kissel, 2011), where it performs numerous key functions including; RNA metabolism, mRNA regulation, endocytic trafficking and development of neuromuscular junction (NMJ) (Bowerman et al, 2017), yet it remains unclear why SMA pathogenesis is specific towards motor neurons.

SMA is broadly divided into two categories – proximal SMA and distal SMA. Proximal SMA is the most common form, accounting for 95% of all cases, and generally manifests during infancy or early childhood with muscle weakness primarily affecting the proximal regions (Farrar & Kiernan, 2015). In contrast, distal SMA is less common with symptoms progressing slower and muscle weakness affecting the distal regions, manifestation occurs during childhood but often progresses into adulthood (Farrar & Kiernan, 2015). Clinically, SMA is categorised into five types (types I-IV and a neonatal type 0) based on disease severity, age of onset and motor function (Table 1), with type I and type IV being the most severe and least severe, respectively (Kolb & Kissel, 2015).

Table 1. SMA is clinically divided into four types based on the severity of symptoms, age of onset, and maximum motor function attained.

Type of SMA	Clinical diagnosis	Age of onset	Motor function achieved
0 (severe infantile)	-	Prenatal	Decreased foetal movements <i>in utero</i> , joint abnormalities, hyporeflexia present
I (infantile)	Werdnig-Hoffman disease	0 – 6 months	Poor head control, inability to sit upright, inability to walk, hypotonia present
II (intermediate)	Dubowitz disease	6 – 18 months	Independent head control, able to sit upright independently, unable to walk independently, limited hypotonia
III (juvenile)	Kugelberg-Welander disease	12 months +	Able to walk independently, wheelchair assistance required later in childhood, no hypotonia
IV (adult-onset)	Adult-onset	Adult	Mild muscle weakening during adulthood, reduced fine motor control, wheelchair assistance may be required

1.2 – Molecular Genetics of SMA

The SMN protein is encoded by the *Survival Motor Neuron (SMN)* locus (5q13) (Lefebvre et al, 1995), which resides within an inverted duplication of a 500kb element within this region. Humans possess two *SMN* copies: a telomeric copy (*SMN1*) and a centromeric copy (*SMN2*) (Lefebvre et al, 1995; Kolb & Kissel, 2011). At the genomic level, the two *SMN* genes are largely identical; sharing a high degree of sequence homology and possessing equivalent promoter sequences giving rise to similar mRNA transcripts (Boda et al, 2004; Monani, 2005). The two *SMN* genes differ only by 5 transcriptionally silent nucleotide changes (Monani et al, 1999).

The functional difference between the two genes is a C-T substitution within exon 7 of *SMN2*, which decreases the amount of exon 7 incorporated into the *SMN2* transcript (Burghes & Beattie, 2009; Kolb & Kissel, 2015). The *SMN1* gene produces a single transcript exclusively encoding the full-length SMN protein (FL-SMN), whereas the *SMN2* gene produces two different transcripts due to alternative splicing, FL-SMN and a truncated protein transcript encodes a truncated protein of diminished function and stability, termed SMN Δ 7 (SMN Δ 7) (Lorson, Hahnen, Androphy & Wirth, 1999; Monani et al, 1999; Burghes & Beattie, 2009). As a consequence of alternative splicing, the major *SMN2* transcript encodes a truncated protein SMN Δ 7 whilst the minor transcript continues to produce FL-SMN identical to that of the *SMN1*

gene product (Burghes & Beattie, 2009) (Figure 1). The majority of the *SMN2* transcripts, accounting for 90% of the total gene product, skip exon 7 during transcription and are thus unable to produce a complete complement of the FL-SMN protein (Kolb & Kissel, 2011).

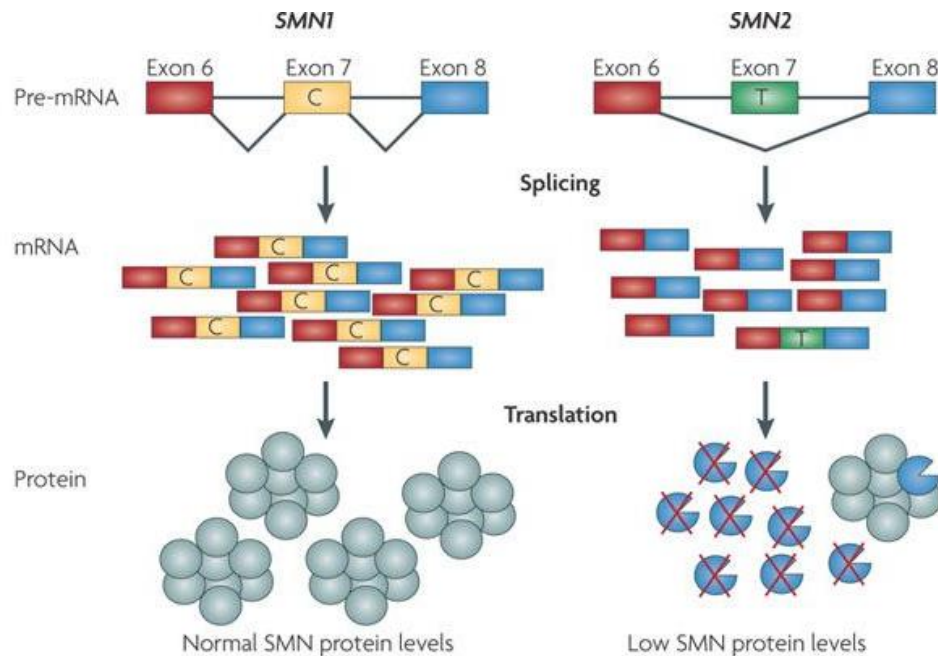


Figure 1. The two *SMN* genes present in humans and their respective gene products. *SMN* protein is produced by two genes – *SMN1* and *SMN2*. *SMN1* produces the full length *SMN* protein whereas the *SMN2* gene produces two different transcripts as a result of alternative splicing. Most of these transcripts contain a premature stop codon and thus encode a truncated protein, which is eventually degraded. Consequently, only a small percentage of healthy *SMN* protein is produced from *SMN2* (Image taken from Burghes & Beattie, 2009).

Presence of the C-T substitution in *SMN2* results in the introduction of a premature stop codon at position +6 of exon 7 which alters a splice consensus site, causing the subsequent exclusion of exon 7 from the *SMN2* mRNA transcript (Kolb & Kissel, 2015). Unlike FL-SMN, *SMNΔ7* lacks the ability to oligomerise correctly, both with itself and other binding partners, and is eventually degraded by the proteasome (Burghes & Beattie, 2009). Introduction of the C-T substitution alters splicing regulatory elements in *SMN2* (Figure 2). Exonic splicing enhancers (ESE) and exonic splicing silencers (ESS) are amongst such elements which enhance and suppress exon inclusion, respectively (Lodish et al, 2008).

Initially it was thought that an ESE was present within *SMN2* which promoted binding of the serine-arginine rich (SR) protein AS/SF2 resulting in mRNA splicing, the C-T substitution disrupted this sequence and caused aberrant splicing (Cartegni & Krainer, 2002). It is now understood that the C-T substitution modifies the pre-existing ESE and converts it into an ESS element. The ESS has a high affinity for the heterogenous ribonucleoprotein hnRNP A1, a negative regulator of splicing. Binding of hnRNP A1 results in the exclusion of exon 7 from the *SMN2* mRNA transcript by repressing normal spliceosome activity (Kashima et al, 2007).

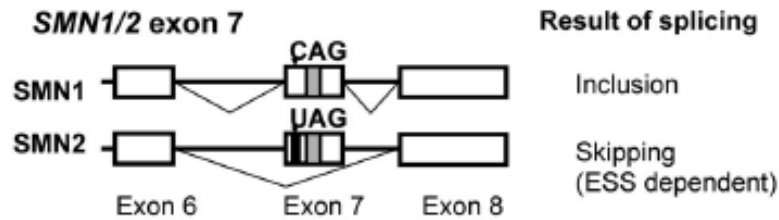


Figure 2. Splicing regulatory sequences are affected by the C-T substitution in *SMN2*. *SMN1* does not possess the C-T substitution and is correctly spliced. Presence of the C-T substitution in *SMN2* creates an ESS element at the 5' end of exon 7 which results in its exclusion from the mRNA transcript (Image adapted from Kashima et al, 2007).

SMA arises due to the homozygous disruption of the *SMN1* gene (Lefebvre et al, 1995), loss of *SMN1* results in a global decrease in the level of the SMN protein. However, *SMN2* however is unaffected and continues to produce a low level of SMN protein. Patients who lack *SMN1* are therefore dependant on the endogenous SMN protein produced by *SMN2*, and consequently, the low amounts produced are inadequate to prevent the onset of SMA (Burghes & Beattie, 2009; Kolb & Kissel, 2011; Kolb & Kissel, 2015).

1.3 – The SMN Protein

The SMN protein is ubiquitously expressed in the nucleus and cytoplasm across all tissues, yet despite the widespread expression pattern, it is unknown why SMA disease pathology is restricted to motor neurons (Monani, 2005). SMN has a well characterised role in the assembly of the eukaryotic spliceosome complex however, it remains elusive as to why SMN depletion is specific towards motor neurons. The issue is complicated further by the myriad of secondary functions performed by SMN, making it difficult to pinpoint the precise molecular mechanisms responsible for the disease onset (Hosseinibarkooie, Schneider, & Wirth, 2017).

SMN itself is a 32kDa multidomain protein encoded by 8 exons, consisting of 294 amino acid residues which generates four structurally distinct domains (Figure 3) (Renvoise et al., 2006). The protein domains include an N-terminal lysine (K)-rich domain, consisting of a conserved K-rich sequence which facilitates RNA binding; a Tudor domain which binds arginine-glycine (RG) motifs present in protein involved in RNA metabolism; a proline (P)-rich domain enabling interaction with actin-binding proteins; and a C-terminal tyrosine-glycine (YG)-box domain which enables self-oligomerisation.

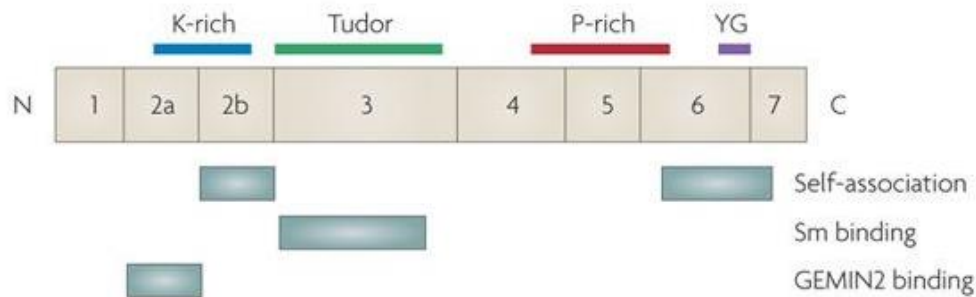


Figure 3. The domain architecture of the SMN protein. From the N to C terminus – a K-rich domain (blue) involved in RNA binding; a Tudor domain (green) to facilitate binding with proteins involved in RNA metabolism; a P-rich domain (red) that interacts with actin-binding proteins and a YG box (purple) which enables self-association (Image taken from Burghes & Beattie, 2009).

The primary role of the SMN is the assembly of the spliceosome machinery in eukaryotic cells, where it functions in the biogenesis of small ribonuclear proteins (snRNP's) which are essential for the splicing of pre-mRNA into mature mRNA (Pellizzoni, Yong & Dreyfuss, 2002; Gubitz, Feng & Dreyfuss, 2004). In the nucleus, SMN forms a stable multimeric complex (termed the SMN complex) through self-oligomerisation and association with Gemin 2-8, unrip and ATP (Battle et al., 2006); Kolb, Battle & Dreyfuss, 2007). Each snRNP consists of a single small nuclear RNA (snRNA) molecule (Including U1, U2, U4, U5 and U6) and several Sm proteins arranged in a heptameric ring (Otter et al, 2007). The SMN complex functions in the ATP-dependant assembly of the snRNP from these components. The Sm proteins are arranged as a heptameric ring around a highly conserved sequence motif in the snRNA known as the Sm site, the SMN complex then binds the components together forming the active snRNP (Figure 4) (Pellizzoni et al, 2002; Kolb, Battle & Dreyfuss, 2007).

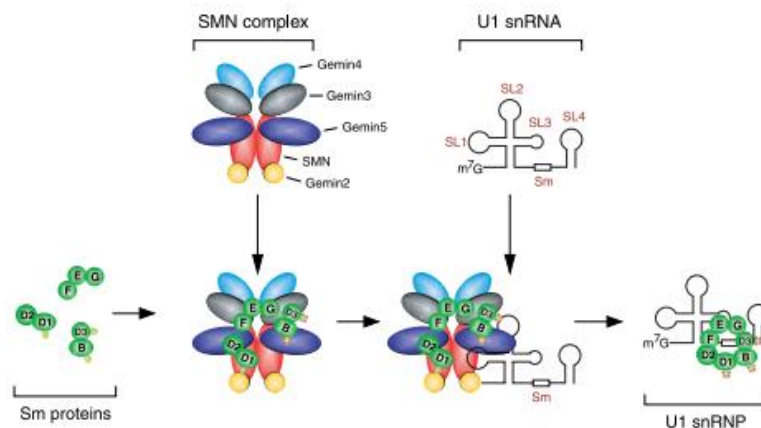


Figure 4. The activity of the SMN complex in the assembly of the snRNP spliceosome machinery. Each active snRNP contains a single snRNA (U1 in this example) and several Sm proteins arranged in a ring around the Sm site of the snRNA. The SMN complex catalyses the binding of these two core components to form the snRNP in an ATP-dependant manner (Image taken from Pellizzoni et al, 2002).

In line with its canonical role in snRNP assembly, SMN has been shown to localise in the nucleus as structures known as Gems (Gemini bodies) (Bowerman et al, 2017). SMN has also been shown to localise in the cytoplasm, axons and synapses of neuronal cells (Figure 5) where several secondary functions have also been documented (Table 2), including: RNA regulation and transport, actin cytoskeletal dynamics, endocytic trafficking, axonal growth and neuronal development (Hosseinibarkooie et al, 2017).

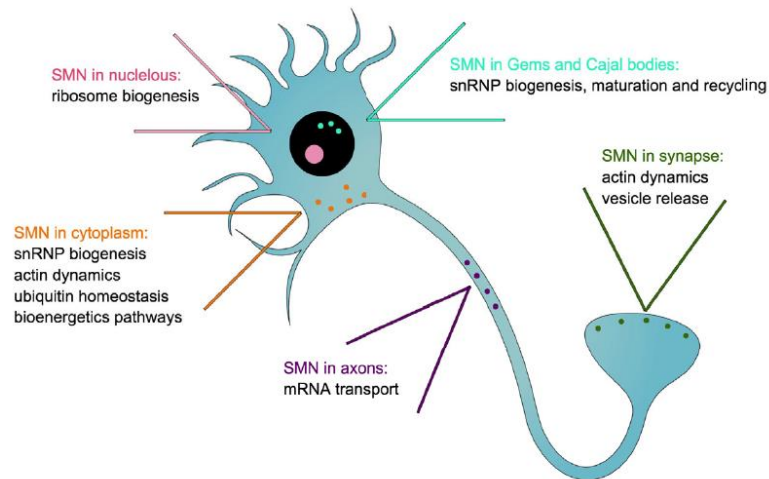


Figure 5. The localisation of the SMN protein in neuronal cells. SMN primarily localises in the nucleus as gems as part of the SMN complex. SMN also localises to the cytoplasm, axons and synapses where it performs a range of secondary functions; notably in neuronal development, endocytic trafficking and cytoskeletal dynamics (Image taken from Bowerman et al, 2017).

Table 2. An overview of the different functions performed by the SMN protein and its protein interactions.

Cellular pathway	SMN function	Protein interactions	References
snRNP biogenesis	Assembles snRNP's	Gemins; Stasimon	Lotti et al. (2012)
RNA transport & regulation	Binds mRNA & localisation; Interaction with RNA binding proteins	hnRNPs; PTEN; HuD	Akten et al. (2011), Ning et al. (2010)
Endocytic trafficking	Synaptic vesicle recycling; Regulates synaptic transmission	PLS3; NCALD	Oprea et al. (2008), Ackermann et al. (2013), Hosseinibarkooie et al. (2016), Riessland et al. (2017)
Cytoskeletal dynamics	Interaction with β -actin; Interactions with actin binding proteins	Profilin; PLS3; NCALD; CORO1C	Oprea et al. (2008), Ackermann et al. (2013), Hosseinibarkooie et al. (2016), Riessland et al. (2017), Giesemann et al. (1999)
Microtubule dynamics	Regulation of microfilaments	Tubulin, Strathmin, CDK5, Tau	Fuller et al. (2015), Wen et al. (2010), Miller et al. (2015)
Proteostasis	SMN depletion decreases levels of ubiquitination proteins	UBA1	Wishart et al. (2014)

SMN is known to translocate between the nucleus and cytoplasm where it is required for the transport of mRNA, this is particularly important in neuronal cells, where it sustains correct neuronal development (Fallini et al, 2012). SMN binds RNA via its lysine-rich domain and has been implicated in the localisation of β -actin mRNA to the axonal growth cones of motor neurons, which is important for correct axonal development and guidance (Rossol et al, 2003). SMN is also capable of interacting with other RNA-binding proteins through interactions with the Tudor domain. Binding with these proteins, is known to influence the levels of their target mRNAs in the axonal compartment. The interaction of SMN with β -actin provided the first evidence that SMN is also involved in actin cytoskeletal dynamics (Rossol et al, 2003). Through its proline-rich domain SMN is capable of interacting with actin binding proteins profilin I and II where they co-localise in the cytoplasm (Bowerman, Shafey, & Kothary, 2007). This binding was found to modulate the inhibitory effects of profilin on actin polymerisation,

possibly by modulating the ratios of F/G actin microfilaments controlling axon morphology (Bowerman, et al., 2009). Proteomic studies have revealed that the levels of Ubiquitin Like Modifier Activating Enzyme 1 (UBA1), a ubiquitin activating enzyme, are reduced when SMN is depleted. Reduced levels of UBA1 are thought to disrupt proteasome degradation in SMA and perturb axon morphology (Hosseinibarkooie et al, 2017).

Recent studies using a *Caenorhabditis elegans* and other SMA mammalian models have demonstrated that endocytic pathways are perturbed in SMA. The *C. elegans* SMA model was used to demonstrate that SMN-1 depletion resulted in decreased neurotransmitter release and abnormal localisation of endocytic proteins (Dimitriadi et al, 2016). This indicates that SMN depletion impairs endocytic trafficking and perturbs synaptic vesicle recycling. Furthermore, studies in mice and zebrafish have shown that knockdown of neurocalcin delta (NCALD) ameliorated disease-associated SMA phenotypes by restoring endocytic function (Riessland et al, 2017). Taken together, these results clearly demonstrate that endocytic pathways are involved in SMA pathology.

Due to the vast array of functions carried out by SMN two hypotheses have emerged which attempt to explain the pathogenesis of SMA (Burghes & Beattie, 2009). The first hypothesis is in line with the canonical role of SMN and suggests the global decrease in SMN prevents the formation of the SMN complex. Subsequently, that interferes with splicing of mRNA transcripts required for correct motor neuron development. The second hypothesis encompasses the other SMN functions, suggesting that one or more of these secondary roles may be disrupted due to SMN depletion, ultimately leading to the gradual deterioration of motor neurons (Hosseinibarkooie et al, 2017).

Despite the genetic components underlying SMA being very well characterised, the precise role of the SMN protein in the pathology of SMA remains unclear. An increasing body of evidence is beginning to demonstrate that the secondary functions of SMN are disrupted in SMA, supporting the notion that SMA pathogenesis may not be restricted to any single role of SMN.

1.4 – Genetic Modifiers of SMA

Genetic modifiers are genes that modulate the severity of a disease phenotype by altering the expression of downstream genetic targets at different loci. *SMN2* was the first identified modifier of SMA (Wirth et al, 2006) due to its variable copy number (Lefebvre et al, 1997), as patients who possess more *SMN2* copies produce a larger amount of SMN and experience milder SMA symptoms (Wirth et al, 2006; Kolb & Kissel, 2015). In this manner, *SMN2* acts as a genetic modifier for SMA by directly increasing the amount of functional SMN produced, thus modulating the SMA severity (Wirth et al, 2006; Wirth 2017). In addition, several other SMA genetic modifiers have been identified in various SMA model systems (Table 3); with *PLS3* and *NCALD* being the only ones identified in humans.

Table 3. An overview of SMA genetic modifiers.

Genetic Modifier	Protein	Cellular Function	Effect on SMA Phenotype	Reference
<i>SMN2</i>	Survival Motor Neuron	Assembly splicing machinery	Increasing copy number directly modulates severity	Wirth et al, 2006
<i>PLS3</i>	Plastin 3	Actin bundling	Overexpression rescues SMN depletion defects by restoring axon length and NMJ functionality	Oprea et al., 2008
<i>NCALD</i>	Neurocalcin Delta	Neuronal calcium sensor	Knockdown ameliorates SMA phenotypes by restoring endocytic defects	Riessland et al, 2017
<i>PTEN</i>	Phosphatase and Tensin Homology	Regulates AKT signalling	Overexpression improves lifespan	Little et al, 2015
<i>ATF6</i>	Activating Transcription Factor 6	Unfolded protein response	Knockdown rescues SMN depletion defects	Wirth et al, 2017
<i>ACTN</i>	Actinin	Actin filament attachment	Knockdown rescues SMN depletion defects	Wirth et al, 2017
<i>AGRN</i>	Agrin	Neuromuscular junction development	Overexpression rescues SMN depletion defects	Boido et al, 2018
<i>ZPR1</i>	Zinc Finger Protein 1	Facilitates mRNA binding of SMN complex	Overexpression rescues SMN depletion defects	Ahmad et al, 2012

Besides *SMN2*, *Plastin 3* (*PLS3*) was the first SMA genetic modifier that was discovered in humans. It was found that *PLS3* expression levels were elevated in asymptomatic females harbouring the same *SMN1* and *SMN2* alleles as their symptomatic siblings (Oprea et al, 2008). *PLS3* encodes a calcium-dependant actin binding protein which has an important role in axon growth by controlling actin cytoskeletal dynamics by bundling F-actin filaments and thus controls the F/G actin ratio in developing axons. Oprea and colleagues (2008) demonstrated that *PLS3* overexpression significantly restored the axon length in motor neurons using a severe SMA mouse model carrying two human *SMN2* copies. Axon length

restoration was attributed to the increased levels of F-actin required for axonogenesis (Oprea et al, 2008). A subsequent genetic screen identified PLS3 as a cross-species invertebrate SMN loss of function modifier, where knockdown of the PLS3 ortholog in *Caenorhabditis elegans* and *Drosophila* SMA models rescued SMN neuromuscular defects (Dimitriadi et al, 2010). In addition, an independent study demonstrated that PLS3 overexpression also restored motor neuron and NMJ functionality, but not lifespan, in a severe SMA mouse model (Ackermann et al, 2013). Furthermore, using a viral vector to deliver PLS3, it was shown that survival of an intermediate SMA mouse model was significantly extended and, when used in conjunction with an SMN increasing ASO, also increased lifespan in a severe SMA mouse model. It is of note that PLS3 overexpression alone is not sufficient to completely rescue SMN depletion defects (Kaifer et al, 2017).

Neurocalcin delta (NCALD) encodes a neuronal calcium sensor and has recently been identified as another SMA genetic modifier. It was found that knockdown of NCALD, a negative regulator of endocytosis, ameliorated disease-associated SMA phenotypes (Riessland et al, 2017). In the absence of Ca^{2+} NCALD binds clathrin, a synaptic vesicle coat protein required for vesicle recycling thereby preventing coating of synaptic vesicles and acting as a negative regulator of endocytosis. SMN depletion reduces voltage-dependant Ca^{2+} influx, as a result the levels of intracellular Ca^{2+} decrease and NCALD binds clathrin, inhibiting the coating of synaptic vesicles and prevents their recycling at the NMJ (Riessland et al, 2017). Using mice and zebrafish SMA models, it was shown that knockdown of NCALD ameliorated disease-associated SMA phenotypes by restoring endocytic function; synaptic vesicle endocytosis was restored in mice NMJs, while axonogenesis defects were restored in zebrafish (Riessland et al, 2017). Furthermore, knockout of the *Sac6p*, the yeast *Plastin* ortholog, resulted in impaired endocytosis (Kübler & Riezman, 1993) and PLS3 overexpression has been shown to rescue endocytic impairments in the NMJ of SMA mouse models (Hosseini et al, 2016).

Overall, cross-species genetic modifiers hold promising potential for therapeutic applications in SMA, the role of *SMN2* is clear however *PLS3* and *NCALD* remain the focal point of current research. Impaired endocytic pathways have been implicated in the pathology of SMA and altered expression of both PLS3 and NCALD has been shown to restore endocytic defects in various mammalian SMA models. Taken together these results clearly demonstrate that endocytic pathways are involved in SMA pathology, highlighting the need for further research.

1.5 – SMA Therapeutic Strategies

To date, there is only a single treatment available for SMA. Nusinersen (Spinraza) became the first FDA approved drug for SMA treatment and was released in 2017 (Ottensen 2017), despite the causative gene being discovered 10 years earlier. Most SMA therapeutics are aimed at increasing the levels of FL-SMN produced either, by exogenously expressing *SMN1* or by increasing the levels of FL-SMN produced from *SMN2* (Wood, Talbot, & Bowerman, 2017).

Nusinersen, product of these efforts, is an antisense oligonucleotide (ASO) treatment which works by increasing the amount of *SMN2* transcripts that include exon 7 (Ottensen, 2017). An important sequence termed intron splicing silence N1 (ISS-N1), was discovered within intron 7 of *SMN2* which further promotes exclusion of exon 7 from the transcript (Singh et al, 2006).

Nusinersen binds to, and inhibits, ISS-N1 thereby promoting the inclusion of exon 7 in the *SMN2* transcripts (Goodkey, Aslesh, Maruyama & Yokota, 2017; (Son & Yokota, 2018)

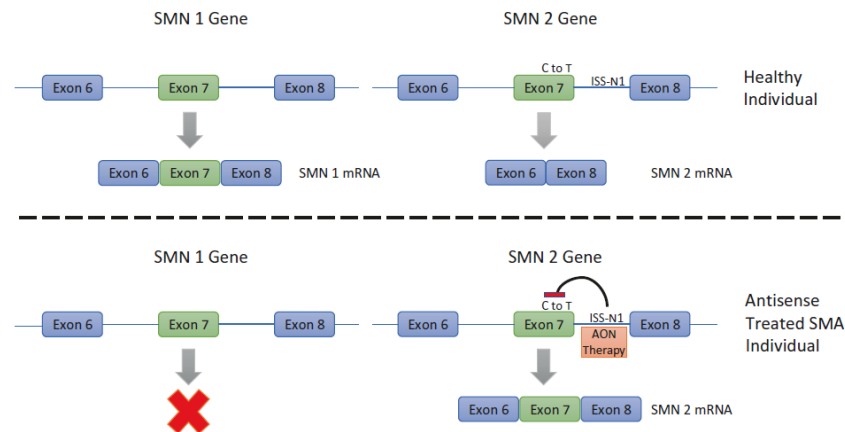


Figure 6. Nusinersen promotes exon 7 inclusion in *SMN2* transcripts by inhibiting ISS-N1. Healthy individuals possess a full complement of SMN protein from the *SMN1* gene and a partial complement from aberrantly spliced *SMN2*. SMA patients are reliant on the low levels of SMN protein produced from *SMN2*. Nusinersen inhibits ISS-N1 in *SMN2* and promotes exon 7 inclusion, thus directly increasing the levels of FL-SMN produced (Image taken from Goodkey et al, 2017).

In addition to Nusinersen, other SMA therapeutic strategies have been described, these other strategies focus on increasing the levels of FL-SMN by improving *SMN2* promoter activation, gene replacement of functional *SMN1* and neuroprotection mediated by small molecules (Bowerman et al, 2017). These strategies primarily focus improving the genetic defects of SMA. In line with these therapies novel genetic modifiers hold promising potential for further therapeutic treatment options, while modulation of novel pathways disrupted in SMA such as autophagy may also provide potential therapeutic targets.

1.6 – The Role of Autophagy in SMA

Autophagy is a vital process for the maintenance of cellular homeostasis under physiological conditions, particularly in motor neurons, where it is frequently disrupted in a range of neurodegenerative disorders. Autophagy is now emerging as a popular topic of SMA investigation to progress the understanding of disease mechanisms and identify potential therapeutic targets.

Autophagy is a highly conserved lysosomal degradation pathway which is vital for maintaining cellular homeostasis by the removal and recycling of damaged cytoplasmic components which are otherwise too large to be degraded by the proteasome system (Reggiori & Klionsky, 2002; Mizushima & Komatsu, 2011). These components are typically protein aggregates but also include aging or dysfunctional organelles and other larger molecules such as lipids and infectious particles (Klionsky & Emr, 2000; Levine & Klionsky, 2004; Levine, Mizushima & Virgin, 2011; Kuo, Hansen & Troemel, 2017).

The autophagic pathway is broadly divided into three classifications; macroautophagy, microautophagy and chaperone-mediated autophagy (Mizushima, 2007) (Figure 6). Each type results in the degradation of cytoplasmic components, mediated by the lysosome, however

the mode of delivery differs (Parzych & Klionsky, 2014). Macroautophagy involves the formation of an intermediate double membrane vesicle which engulfs bulk cytoplasmic material and transports it to the lysosome (Mehrpour, Esclatine, Beau & Codogno, 2010). Microautophagy occurs when the lysosome itself directly takes up smaller cytoplasmic material, the lysosomal membrane invaginates to take up cytoplasmic cargo via endocytosis (Li, Li & Bao, 2012). Chaperone-mediated is distinct from the other types of autophagy as the cytoplasmic material being degraded is not transported via vesicle structures. Instead, the cytoplasmic cargo is bound to chaperone proteins which are recognised by receptors on the lysosome, receptor binding facilitates the lysosomal import of the cargo (Kaushik & Cuervo, 2012). In contrast to macroautophagy and microautophagy, chaperone cargo binding enables degradation of specific types of cytoplasmic material and is thus a form of selective autophagy (Wang, Peng, Ren & Wang, 2015).

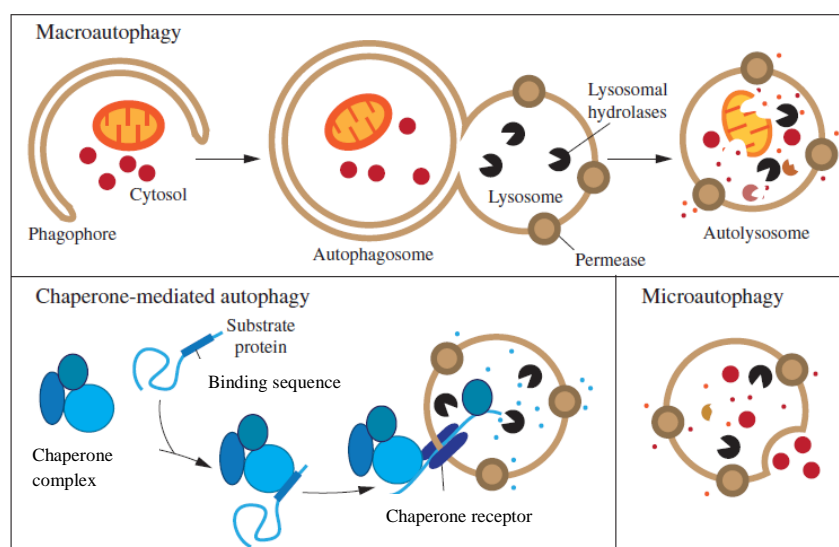


Figure 7. The different types of autophagic pathways. Macroautophagy is characterised by the formation of an intermediate double membrane (autophagosome) which fuses with the lysosome (autolysosome), to degrade cellular cargo. Microautophagy occurs when the lysosomal membrane itself invaginates to facilitate cargo uptake and degradation. Chaperone-mediated autophagy is a selective form of autophagy where cargo is bound to chaperone proteins ultimately facilitating binding with the lysosome and enabling cargo translocation into the lysosome (Image adapted from Parzych & Klionsky, 2014).

Autophagy is a ubiquitous catabolic process occurring at a constitutive level in the cell where it plays an important role in cell survival by maintaining cellular integrity in the form of proteostasis (Levine & Kroemer, 2009). Autophagy is a highly regulated process and is upregulated in response to a wide variety of cellular stresses including: starvation, temperature, oxidative stress, infection and growth and development (Moreau, Luo & Rubinsztein, 2010; Levine et al, 2011). When upregulated, autophagy acts as a protective process to promote survival however, impaired or excessive autophagy can be detrimental resulting in accumulation of protein aggregates – a typical feature of many neurodegenerative disorders (Nixon, 2013; Martinez-Vincente, 2015). This pathway is known to be perturbed in several other neurodegenerative disorders including: Alzheimer’s disease (AD), Parkinson’s disease (PD), Amyotrophic Lateral Sclerosis (ALS) and Huntingdon’s disease (HD) (Cherra & Chu, 2008; Nah, Yuan & Jung, 2015; Mis, Brajkovic, Frattini, Di Fonzo & Corti, 2016).

Functional autophagy is essential for preventing the accumulation of misfolded protein aggregates, a hallmark trait of the majority of neurodegenerative diseases. When impaired, autophagy fails to clear protein aggregates ultimately leading to neurodegeneration (Yang et al, 2015). The genes controlling the autophagy, termed *ATG* genes, were originally identified and characterised through a series of genetic screens in yeast (Takeshige, Baba, Noda & Oshumi, 1992; Tsukada & Oshumi, 1993; Thumm et al, 1994) and have provided the basis for elucidating the various autophagic pathways. Many of the genes identified through these genetic screens possess orthologs in invertebrates and mammals (Table 4), demonstrating the significance and conservation of autophagy (Oshumi, 2014).

Macroautophagy (herein referred to as autophagy) is the main pathway used for the clearance of aggregated protein and damaged organelles as it is capable of degrading material in bulk, and in a non-selective manner (Parzych & Klionsky, 2014). Autophagy is characterised by the formation of a large double membrane vesicle structure known as the autophagosome. The cytoplasmic material to be degraded is completely sequestered by a growing nascent membrane, termed the phagophore, which fuses with itself to form the autophagosome. Upon completion, the autophagosome fuses with a lysosome, forming an autolysosome, where the lysosomal enzymes facilitate degradation of the sequestered material (Glick, Barth & Macleod, 2010). Autophagy is governed by a series of protein complexes (Table 4) and occurs across four distinctive stages – (i) autophagy induction, (ii) vesicle nucleation, (iii) vesicle elongation, (iv) lysosomal fusion and degradation (Figure 7).

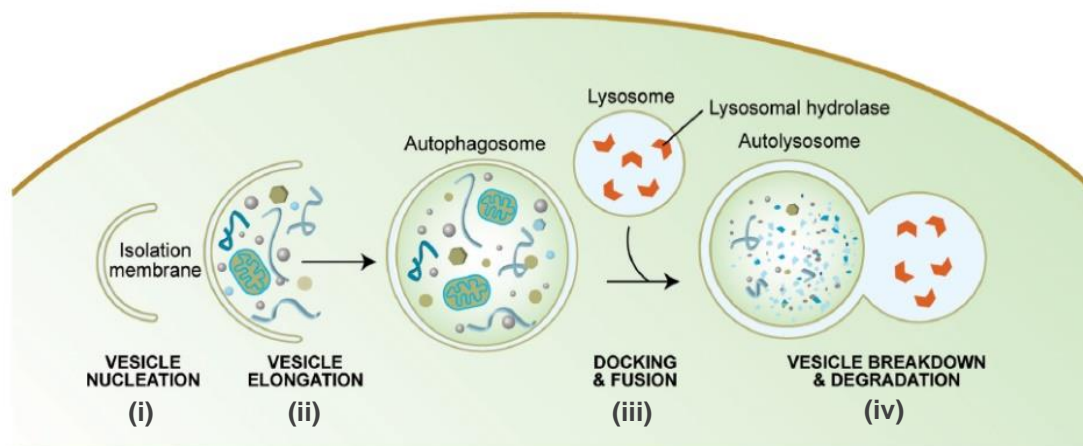


Figure 8. The main cellular events of the autophagy process. The pathway starts with the formation of an isolation membrane (phagophore) which eventually sequesters the cytoplasmic material to be degraded, forming the autophagosome. The autophagosome subsequently fuses with a lysosome, forming an autophagolysosome where the material is finally degraded by lysosomal digestive enzymes (Image taken from Meléndez & Levine, 2009).

The process begins with the formation of an isolation membrane termed the phagophore. In yeast, this membrane is formed at a cytoplasmic structure known as the phagophore assembly site (PAS), however there is no evidence to suggest a PAS is present in mammalian cells. Instead, the phagophore is thought to originate primarily from the ER membrane at structures termed omegasomes (Mizushima & Komatsu, 2011).

Induction of autophagy is controlled by the first protein complex, ULK1/2-Atg13-FIP200 (homologous to the yeast Atg1-Atg13-Atg17 complex) (Glick et al, 2010). This induction complex is Ser/Thr protein kinase regulated by the mammalian target of rapamycin complex 1 (mTORC1) kinase which inactivates the complex via phosphorylation of ULK1/2 under normal conditions. Upon induction of autophagy, mTORC1 is inhibited and dissociates from the induction complex, resulting in its dephosphorylation and enabling it to associate with the ER where it recruits the second protein complex (Parzych & Klionsky, 2014).

Vesicle nucleation is controlled by the second protein complex, a class III phosphatidylinositol 3-kinase (PI3K) comprising VPS43-P150-BECN1 (homologous to the yeast Vps34-Vps15-Atg6/Vps30 complex) (Glick et al, 2010). The class III PI3K complex associates with ATG14 which directs its localisation to site of phagophore assembly, following its localisation to the phagophore the PtdIns3K complex produces phosphatidylinositol-3-phosphate (PI3P) which begins phagophore elongation (Parzych & Klionsky, 2014; Yin, Pascual & Klionsky, 2016). The PI3K complex is regulated by the activity of BECN1 (Atg6/Vps30 in yeast) which interacts with ATG14 and enables it to associate with the PI3K complex. BECN1 is normally bound by BCL2 (an antiapoptotic protein), preventing its interaction with ATG14 and inhibiting autophagy, this binding is reversed upon autophagy induction (Yin et al, 2016).

Vesicle elongation is controlled by two ubiquitin-like protein conjugation systems – ATG12-ATG5-ATG16L (homologous to the yeast Atg12-Atg5-Atg16 complex) conjugation system and the LC3 (homologous to the yeast Atg8) system (Glick et al, 2010). In the first system, ATG12 is covalently linked to ATG5 by the activity of ATG7 (E1-like activating enzyme) and ATG10 (E2-like conjugating enzyme). ATG16L binds to ATG5 and causes dimerization of the complex, this complex then associates with the phagophore to promote membrane expansion (Yu, Chen & Tooze, 2017). In the second system, LC3 is cleaved by ATG4 (a cysteine protease) which exposes a glycine residue at the C terminus (LC3-I). ATG7 activates cleaved LC3-I and transfers it to ATG3 (another E2-like conjugating enzyme). Finally, the C-terminal glycine is conjugated to the lipid phosphatidylethanolamine (PE) (LC3-II) which is thought to be facilitated by the action of the ATG12-ATG5-ATG16L complex acting as a E3-like ligase, LC3-II is then incorporated into the phagophore to expand the membrane until the membranes fuse forming the autophagosome (Yu et al, 2017).

Upon maturation, the autophagosome is able to dock with the lysosome through the action of P62/SQSTM1 (Glick et al, 2010; Mizushima & Komatsu, 2011). P62 acts as an adaptor protein located in the lysosome membrane and recognises the LC3 protein in the autophagosome membrane. Binding of these proteins facilitates the docking of the two structures and initiates their fusion, thereby enabling the release of the autophagosome cargo into the lysosome lumen for degradation and recycling via the action of hydrolytic enzymes (Rusten & Stenmark, 2010; Liu et al, 2016).

Table 4. An overview of the protein complexes and components involved in the autophagic pathway and the genes involved in the complex.

Protein Complex	Function	Autophagy Genes Involved	Saccharomyces cerevisiae Ortholog	Caenorhabditis elegans Ortholog
Autophagy induction complex	Ser/Thr kinase. Induces autophagy in response to cellular signals	<i>mTORC1</i> <i>Ulk-1/Ulk-2</i> <i>Atg13</i> <i>FIP200</i> - - - - <i>Atg101</i>	<i>TOR1</i> <i>ATG1</i> <i>ATG13</i> <i>ATG17</i> <i>ATG31</i> <i>ATG29</i> <i>ATG11</i> <i>ATG20</i> -	<i>let-363</i> <i>unc-51</i> <i>epg-1/atg-13</i> - - - - -
Vesicle nucleation complex	Class III PI3K. Produces PI3P which begins phagophore elongation	<i>Vps34</i> <i>p150</i> <i>Becn1</i> <i>Atg14</i> <i>WIPI1/WIPI2</i> - <i>Bcl-2</i>	<i>VPS34</i> <i>VPS15</i> <i>ATG6/VPS30</i> <i>ATG14</i> <i>ATG18</i> <i>ATG21</i> -	<i>vps-34</i> <i>vps-15</i> <i>bec-1</i> <i>epg-8</i> <i>atg-18</i> - <i>ced-9</i>
Lipid conjugation complex	Ubiquitin-like conjugation system. Recruits the lipidation complex to expand phagophore.	<i>Atg12</i> <i>Atg5</i> <i>Atg7</i> <i>Atg10</i> <i>Atg16L1/Atg16L2</i>	<i>ATG12</i> <i>ATG5</i> <i>ATG7</i> <i>ATG10</i> <i>ATG16</i>	<i>lgg-3</i> <i>atg-5</i> <i>atg-7</i> <i>atg-10</i> <i>atg-16.1/atg-16.2</i>
Lipidation complex	Ubiquitin-like conjugation system. Promotes phagophore expansion	<i>LC3</i> <i>Atg4</i> <i>Atg7</i> <i>Atg3</i> <i>Atg9</i> - -	<i>ATG8</i> <i>ATG4</i> <i>ATG7</i> <i>ATG3</i> <i>ATG9</i> <i>ATG23</i> <i>ATG27</i>	<i>lgg-1/lgg-2</i> <i>atg-4.1/atg-4.2</i> <i>atg-7</i> <i>atg-3</i> <i>atg-9</i> - -
Autophagosome-lysosome fusion components	Binds LGG-1 in the autophagosome membrane and promotes docking and fusion with the lysosome	<i>p62/SQSTM1</i>	-	<i>sqst-1</i>

An increasing body of evidence suggesting that autophagy, a classical endosomal pathway is disrupted in SMA (Table 5) (Garcera, et al, 2013; Custer & Androphy, 2014; Periyakaruppiyah et al, 2016; Piras et al, 2017). These findings were obtained using a variety of *in vivo* and *in vitro* SMA models, providing new insights into the possible mechanisms of SMA disease pathogenesis and could represent new therapeutic targets.

The first evidence showing autophagy was dysregulated in SMA came from Smn-reduced mice motor neurons. Using the LC3 and Beclin-1 autophagy markers, proteins associated with the autophagosome, it was shown that Smn depletion caused autophagosomes to accumulate in these cells (Garcera et al, 2013). The increase in autophagosomes may be a result of excessive autophagy induction or impaired autophagic flux. The same study used Bafilomycin A1 (BafA1), a known autophagy inhibitor that blocks autophagosome and lysosomal fusion, to demonstrate that flux was unaffected in these cells (Garcera et al, 2013).

An independent study obtained similar results using a cultured SMN-depleted motor neuron cell line (NCS-34) and cultured fibroblasts from SMA patients. Using an LC3 marker, it was demonstrated that autophagosomes accumulated in both cell culture systems. In addition, an LC3 tandem fluorescent marker was used in conjunction with p62, a protein degraded by the fusion autophagosomes and lysosomes, to show that flux was also unaffected in these SMA cell culture models (Custer & Androphy, 2014).

Furthermore, an additional study demonstrated that the number of autophagosomes were increased in spinal cord motor neurons from a postnatal severe SMA mouse model, building on the observation that these structures were observed to be increased in SMN-reduced motor neurons (Periyakaruppiyah et al, 2016). The same study also used a p62 monitoring assay to show that autophagic flux is indeed reduced in cultured SMA mice motor neurons. Modulators of the autophagic pathway were also shown to affect the Smn levels in Smn reduced mice motor neurons; autophagy flux inhibitors (BafA1) and autophagy activators (Rapamycin) reduced and increased these levels, respectively, suggesting the possibility of therapeutic targets (Periyakaruppiyah et al, 2016).

Finally, a recent study has shown that inhibition of autophagy increases lifespan and delays motor neuron degeneration in an intermediate (SMA type II) SMA mouse model (Piras et al, 2017). This study reports that the autophagic markers Beclin 1 and LC3 are increased in the lumbar spinal cords of this model, however the p62 levels were unaffected. These results suggest that autophagy was indeed upregulated due to the increased number of autophagosomes but autophagic flux was unaffected, indicating that autophagy may be destructive in the context of SMA (Piras et al, 2017). In addition, the same study reported that treatment with another autophagy inhibitor (3-methyladenine) decreased the levels of autophagic vesicles and increased the p62 levels. Furthermore, treating the intermediate SMA mice with this inhibitor significantly increased lifespan in this model (Piras et al, 2017; (Piras & Boido, 2018).

Table 5. The current evidence demonstrating autophagic disruptions in SMA disease pathology.

SMA Model System	Autophagic Markers Assessed	Main Findings	Reference
Cultured Smn reduced mice motor neurons	LC3 Beclin-1	Autophagosomes accumulate following Smn depletion; BafA1 treatment increased LC3 levels – indicating flux was unaffected	Garcera et al, 2003
SMN depleted motor neuron cells (NCS-34); Cultured SMA patient fibroblasts	LC3 (tandem fluorescence) p62	Autophagic vesicles accumulate in both cell culture models; autophagic flux was reduced	Custer & Androphy, 2014
Severe SMA mouse model; Cultured Smn reduced mice motor neurons	LC3 p62	Autophagic vesicle levels are increased throughout development; autophagic flux was reduced; BafA1 (autophagy inhibitor) treatment reduced Smn protein levels; Rapamycin treatment (autophagy activator) increased Smn protein levels	Periyakruppiah et al, 2016
Intermediate (SMA type II) mouse model	LC3 Beclin-1 p62	Autophagosomes accumulate due to Smn decrease; autophagy upregulated but autophagic flux unaffected; following 3-methyladenine (autophagy inhibitor) treatment, autophagosomes were reduced and lifespan improved	Piras et al, 2017

In summary, these findings clearly illustrate that autophagy is dysregulated in SMA. However, the exact nature of this disruption and its role in SMA pathogenesis remain unclear. Evidence gained from *in vivo* and *in vitro* SMA models shows that autophagosome formation is upregulated, whilst autophagic flux remains unaffected, suggesting that autophagy inhibition may be an attractive source of novel SMA therapeutics.

1.7 – *Caenorhabditis elegans* as a Model to Study SMA

The free-living soil nematode *Caenorhabditis elegans* is an invertebrate model organism which possesses a range of traits that make it an ideal model to study cellular processes at the whole organism level. *C. elegans* are a hermaphrodite species and are thus easily cultivated and maintained; the animals are transparent, allowing the visualisation of specific cells and sub-cellular structures, and they have a short life cycle of 2.5 days at 25°C (Brenner, 1974). The animals are amenable to genetic analysis, boasting a fully sequenced genome with efficient forward and reverse genetics approaches enabling the genetic characterisation of molecular mechanisms (Riddle, Blumenthal, Meyer & Priess, 1997). Finally, the nematode possess an invariant cell lineage and the developmental fate of all 959 somatic cells have been characterised (Sulston & Horvitz, 1977; Sulston, Schierenberg, White & Thomson, 1983), including the nervous system which comprises 302 neurons. The anatomy of the nervous system and the neuronal circuitry have been completely mapped (White, Southgate, Thomson & Brenner, 1988), thus making *C. elegans* a particularly advantageous model to study neurodegenerative disorders such as SMA.

C. elegans possess a single ortholog of the human *SMN1* gene, termed *smn-1*, which encodes a highly conserved protein to SMN, also termed SMN-1 (Miguel-Aliaga et al, 1999). Depletion of SMN-1 leads to growth defects, sterility and larval lethality (Figure 9). Reminiscent of human disease, diminished SMN-1 also impairs neuromuscular function in locomotion (Briese et al, 2009), making *C. elegans* an attractive model to study SMA disease pathogenesis.

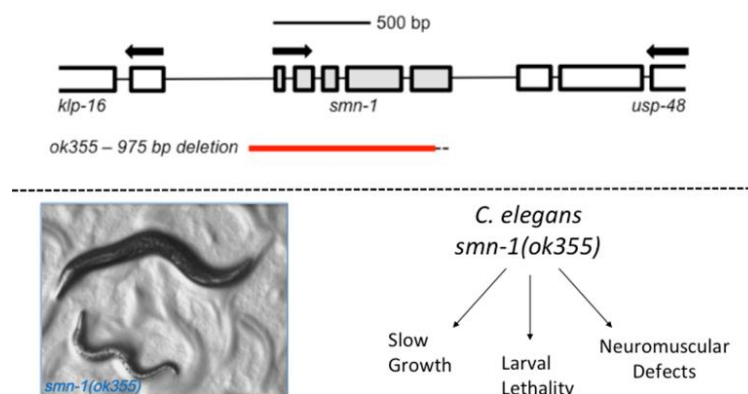


Figure 9. The *C. elegans* loss-of-function SMA model. The *C. elegans* SMA model harbours a 975bp deletion which effectively eliminating *smn-1* gene function. Loss of *smn-1* is accompanied by severe phenotypic defects; *smn-1* loss of function animals (bottom) display slow growth and die during late larval stages compared to wild type age-matched controls (top).

The previously described *C. elegans* SMA model is a loss-of-function model (Figure 9) featuring a 975bp deletion allele (*ok355*) which effectively eliminates most of the gene, causing a complete loss of the *smn-1* function, termed *smn-1(lf)*. Deletion of *smn-1* leads to growth defects, sterility and embryonic lethality, however *smn-1(lf)* animals can survive through early larval stages due to maternal loading of SMN-1. In addition to the aforementioned defects the *smn-1(lf)* animals also possess severe neuromuscular defects which manifest as locomotion and pharyngeal pumping defects (Briese et al, 2009).

Furthermore, many of the yeast *ATG* genes have equivalent orthologs present in *C. elegans* (Table 4), making it an ideal model organism to further study the mechanisms of autophagy in relation to SMA pathogenesis (Zhang et al, 2015). Since the animals are amenable to genetic analysis, powerful reverse genetics approaches can be employed to dissect the mechanism(s) through which autophagic perturbations control SMN function.

1.8 – Project Aims & Objectives

In light of the increasing body of evidence that suggests autophagy is disrupted in SMA (Table 5), we hypothesise that key autophagy regulators may act as putative modifier genes of SMN loss of function defects. Using the powerful genetic tools of *C. elegans* we sought to elucidate the precise cellular and molecular mechanisms underlying SMA disease pathogenesis, with the ultimate goal to identify novel therapeutic avenues for SMA treatment options.

In the present study, we sought to utilise the nematode *C. elegans*, a powerful invertebrate model organism to delineate how autophagic perturbations contribute to SMA pathogenesis. To determine whether autophagic perturbations control SMN neuromuscular function, a reverse genetics approach was used in conjunction with the *C. elegans* SMA model in order to identify novel modulators of SMN function. An RNAi-based genetic screen was conducted to knockdown 22 autophagy orthologs (Table 4) in the *C. elegans* SMA model, a neuromuscular behavioural assay was then employed to determine if knockdown of these genes resulted in the amelioration of the SMN loss of function neuromuscular defects observed in these animals.

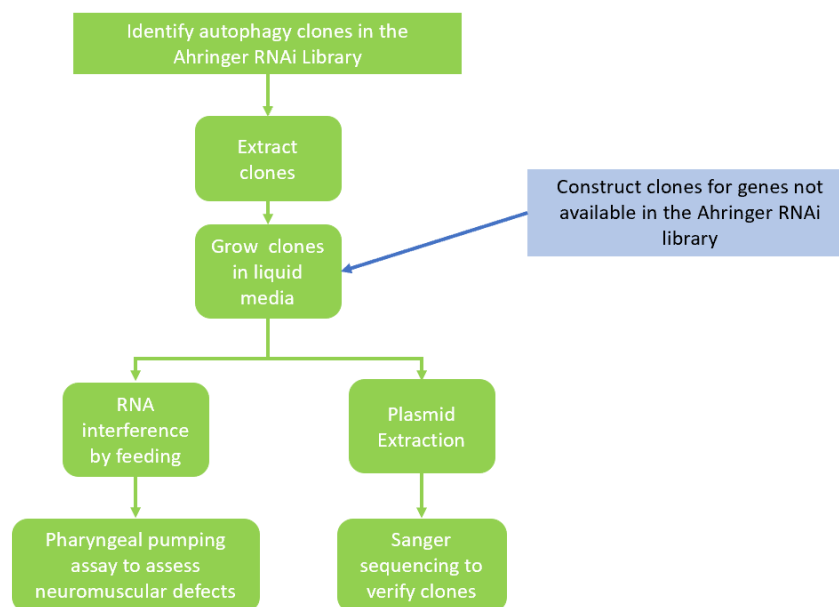


Figure 10. The experimental procedures used in this study to identify putative genetic modifiers of SMN loss of function neuromuscular defects. All known *C. elegans* autophagy orthologs were screened using an RNAi feeding protocol. Knockdown was assessed using a pharyngeal pumping behavioural assay to determine if gene knockdown could modify the defects observed in *smn-1(ok355)* animals.

2 Materials and Methods

2.1 – *Caenorhabditis elegans* strains and maintenance

All *C. elegans* strains were cultivated and maintained at 20°C on nematode growth medium (NGM) plates seeded with OP50 *Escherichia coli* bacteria as previously described (Brenner, 1974). The following strains were used in this work: Bristol N2, LM99 *smn-1(ok355) I/hT2 [bli-4(e937) qIs48 [myo-2p::GFP; pes-10p::GFP; ges-1p::GFP]] (I;III)*, HA1981 (+)/hT2 *[bli-4(e937) qIs42 [myo-2p::GFP; pes-10p::GFP; ges-1p::GFP]] (I;III)*, HA2599 (+)/ht2 *[bli-4(e937) qIs48 [myo-2p::GFP; pes-10p::GFP; ges-1p::GFP]] (I;III)*; *uls72 [pCFJ90(myo-2p::mCherry) + unc-119p::sid-1 + mec-18p::mec-18::GFP]*, HA2623 *smn-1/ht2 [bli-4(e937) qIs48 [myo-2p::GFP; pes-10p::GFP; ges-1p::GFP]] (I;III)*; *uls72 [pCFJ90(myo-2p::mCherry) + unc-119p::sid-1 + mec-18p::mec-18::GFP]*, CB1467 *him-5(e1467)* V. HA2599 was constructed by crossing young adult *him-5* males with L4 *smn-1/hT2; uls72* hermaphrodites, two generations of progeny were validated with PCR genotyping.

C. elegans smn-1(ok355) animals cannot be maintained as homozygotes due to infertility. Therefore, *smn-1(ok355)* animals were maintained as heterozygotes with the *hT2* chromosome balancer which is a translocation of segments from chromosomes I and III (strain LM99) (Briese et al, 2009). The strains HA2599 and HA2623 are specialised neuronal RNA interference (RNAi) sensitive strains. RNAi is systemic in *C. elegans* and targets most tissues with the exception of neurons, vulval tissue, sperm and the pharynx (Conte Jr., MacNeil, Walhout & Mello, 2017). HA2599 and HA2623 possess chromosomally integrated transgenes which express SID-1 in neurons, allowing the uptake of dsRNA and thus enhancing RNAi in neuronal tissues (Calixto, Chelur, Topalidou, Chen & Chalfie, 2010).

2.2 – RNA interference by bacterial feeding

The Ahringer RNAi library is a bacterial feeding library comprising 16,757 clones representing 86% of the *C. elegans* genome (Kamath & Ahringer, 2003; Kamath et al, 2003). Each gene has been cloned into an L4440 feeding vector between two inverted T7 promoters and subsequently transformed into HT115(DE3) *E. coli* bacteria resistant to tetracycline. The L4440 plasmid has isopropyl β-D-1-thiogalactopyranoside (IPTG) inducible T7 promoter system and ampicillin resistance marker. Bacteria expressing double stranded RNA were taken from the Ahringer RNAi library (SourceBioscience) and used to inoculate LB media supplemented with 100µg/mL ampicillin (Sigma-Aldrich) and 12.5µg/mL tetracycline (Sigma-Aldrich) and grown at 37°C and 150 RPM overnight. Following incubation, the culture was supplemented with 50% glycerol (ThermoFisher) and stored at -80°C.

Tetracycline is known to inhibit RNAi in *C. elegans* (Kamath et al, 2001) and thus glycerol stocks were used to inoculate LB media supplemented with 100µg/mL ampicillin and grown at 37°C and 150 RPM overnight. Following incubation, 600µL bacterial culture was seeded onto NGM plates supplemented with 100µg/mL ampicillin and 6mM IPTG (ThermoFisher) and left open under a laminar flow hood to dry for 4 hours followed by 24 hours at room temperature. For each gene under analysis, 10-20 animals were passaged to RNAi plates, the animals were placed at 25°C for 5 hours to lay eggs before being removed from the plates.

Prior to experimentation, each clone was verified by sanger sequencing. Bacteria were taken from glycerol stocks and cultured in LB media supplemented with 100µg/mL ampicillin and 12.5µg/mL tetracycline and grown at 37°C and 150 RPM overnight. Bacterial cells were harvested at 6800xg for 3 minutes, a QIAprep Spin Miniprep Kit (Qiagen) was used to extract plasmid and the L4440 plasmid primers (Table 6) were used for sequencing.

RNAi was facilitated in *C. elegans* according to a bacterial feeding protocol (Timmons & Fire, 1998) where animals ingest HT115 *E. coli* expressing double stranded RNA which spreads throughout the animal and potently silences the corresponding gene (Timmons, Court & Fire, 2001). The effects of RNAi-mediated gene knockdown were assessed in second generation animals using a pharyngeal pumping neuromuscular behavioural assay after 3 days post-hatching (2 days at 25°C followed by 1 day at 20°C) on RNAi plates.

2.3 – Construction of RNA interference feeding clones for *atg-3* and *atg-4.2*

The *C. elegans atg-3* and *atg-4.2* autophagy orthologs were not present in the Ahringer RNAi library and thus RNAi feeding constructs were created via PCR and cloning. Genomic fragments of these genes, encompassing the largest available exons, were derived from an N2 animal lysate using PCR amplification with *atg-3* and *atg-4.2* primers (Table 6) The amplified genomic fragments were purified using a QIAquick PCR Purification Kit (Qiagen) before being subjected to a restriction digest using *XhoI* and *HindIII* restriction endonucleases. The *XhoI/HindIII* restriction products were purified via 0.8% agarose gel electrophoresis and extracted using a QIAquick Gel Extraction Kit (Qiagen) before being subcloned into pL4440 (addgene plasmid #1654), also digested with *XhoI* and *HindIII*, between two inverted T7 promoters in the multiple cloning site. The resulting construct was verified via agarose gel electrophoresis before being used to transform TOP10 *E. coli* via heat shock, the transformants were spread on LB agar with 100µg/mL ampicillin and grown at 37°C overnight. The resulting colonies were verified with colony PCR using the aforementioned primers. Single colonies were used to inoculate LB media with supplemented with 100µg/mL ampicillin and 12.5µg/mL tetracycline and grown at 37°C and 150 RPM overnight. Bacterial cells were harvested at 6800xg for 3 minutes, a QIAprep Spin Miniprep Kit (Qiagen) was used to extract plasmids which were verified via sanger sequencing with L4440 plasmid primers (Table 6) Sequence analysis and alignment was conducted to ensure no mutations were present in the constructs. The RNAi feeding constructs were then transformed into HT115 *E. coli* via heat shock and the transformants were spread on LB agar with 100µg/mL ampicillin and 12.5µg/mL tetracycline and grown at 37°C overnight. Single colonies were used to inoculate LB media supplemented with 100µg/mL ampicillin and 12.5µg/mL tetracycline and grown at 37°C and 150 RPM overnight. Following incubation, the culture was supplemented with 50% glycerol and stored at -80°C.

Table 6. A list of the primer sequences used throughout this study.

Amplification target	Forward primer sequence 5' – 3'	Reverse primer sequence 5' – 3'
L4440 plasmid	ACGACTCACTATAGGGA GAC	GTTGTAAAACGACGGCCAGT
<i>atg-3</i>	TGATCTCGAGTTGTAGTT GAGAAGAAGCCG	TGATAAGCTTCAAGTTGGTGAGC GAATAGA
<i>atg-4.2</i>	TGATCTCGAGAGAAAGT GGTCTTCGCTCG	TGATAAGCTTGCGCACTTGGATG GAGCCTAAAC

2.4 – RNA interference based genetic screen of *C. elegans* autophagy orthologs

10 gravid (+)/*hT2*; *uls72* and 20 *smn-1/hT2*; *uls72* animals were transferred to RNAi plates seeded with a candidate RNAi bacterial feeding clone corresponding to a *C. elegans* autophagy ortholog, or an empty vector control (L4440). The animals were placed at 25°C for 5 hours to lay eggs before being removed from the plates in order to achieve an age matched population. Eggs were allowed to hatch, and animals were maintained on the RNAi bacterial feeding strains for 3 days (2 days at 25°C followed by 1 day at 20°C) before the procedure was repeated with second generation animals. Second generation animals were assessed for neuromuscular defects (pharyngeal pumping) after 3 days post-hatching (2 days at 25°C followed by 1 day at 20°C) on RNAi plates.

2.5 – Pharyngeal pumping neuromuscular behavioural assay

Pharyngeal pumping assays were used to assess the neuromuscular defects in wild type animals derived from the (+)/*hT2*; *uls72* strain, and *smn-1(ok355)* animals derived from the *smn-1/hT2*; *uls72* strain following knockdown of autophagy genes. The average number of pharyngeal pumps per minute was determined after 3 days (2 days at 25°C, 1 day at 20°C) post-hatching on empty vector control and RNAi candidate feeding strains. Animals were recorded using an AxioCam ICc5 mounted on a Zeiss Discovery.V8 stereomicroscope at 126x magnification. Animals were recorded for 10 seconds at a resolution of 1260x930 with an exposure time of 30ms and recordings were slowed before counting pharyngeal pumps. Pharyngeal pumps were scored as a single complete revolution of the pharynx. For each RNAi candidate gene and control, the average number of pharyngeal pumps (\pm S.E.M.) was determined for both genotypes from at least three independent trials ($n \geq 30$ animals in total).

2.6 – Data analysis

All recorded videos from pharyngeal pumping experiments were analysed using Zeiss Zen 2 image processing software equipped with time lapse functionality. Subsequent data analysis was performed using Microsoft Excel and GraphPad Prism 8. SnapGene was used to create plasmid maps for newly generated constructs and for assessing sequence alignments. Pharyngeal pumping statistical analysis was performed using a two-tailed Mann-Whitney *U* test.

3 Results

3.1 – Neuromuscular Behavioural Assay

3.1.1 – *smn-1(ok355)* mutants exhibit pharyngeal pumping defects

The previously described *C. elegans* SMA model has been used to demonstrate that the *smn-1(ok355)* deletion allele results in progressive neuromuscular defects, including drastically decreased rates of pharyngeal pumping (Briese et al, 2009). This model was used herein to verify the pharyngeal pumping characteristics of the *smn-1(ok355)* animals compared to wild type animals. *C. elegans* feed on bacteria via the rhythmic contraction and relaxation of its pharynx, a neuromuscular pump composed of a small discrete subset of muscles and neurons (Trojanowski, Raizen & Fang-Yen, 2016) (Figure 11A). The pharynx pumps continuously as bacteria are ingested and broken down by the grinder; in wild type animals the rate of pharyngeal pumping ranges from 200-250 pumps per minute. In *smn-1(ok355)* animals the rate of pharyngeal pumping significantly declines to 30-50 times per minute, reflecting the progressive neuromuscular defects (Briese et al, 2009; Dimitriadi et al, 2010).

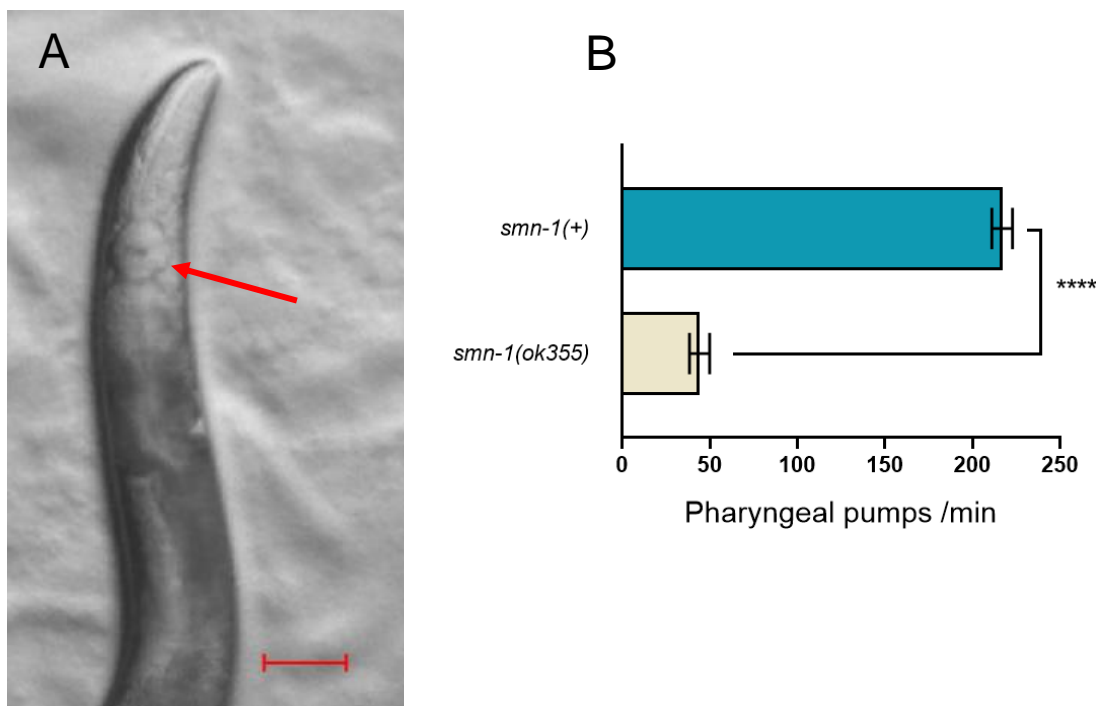


Figure 11. The rate of pharyngeal pumping is significantly decreased in *smn-1(ok355)* animals compared to controls. (A) *C. elegans* feed on bacteria through the pharynx, a neuromuscular pump that continuously contracts and relaxes as the animal captures and grinds bacteria. Pharyngeal pumps were determined by counting complete revolutions of the grinder (indicated by the arrow); scale bar indicates 1000µm. (B) The rates of pharyngeal pumping in *smn-1(ok355)* and *smn-1(+)* control animals were determined at day 3 post hatching on RNAi plates with a bacterial feeding strain expressing L4440 (empty RNAi vector). Fifty animals were scored across 5 independent trials. Error bars display \pm SEM; Asterisks indicate significant difference determined using a Mann-Whitney *U* test, two tailed: * $p < 0.05$, ** $p < 0.001$, *** $p < 0.0001$.

To determine whether these values could be recapitulated, *smn-1(ok355)* and *smn-1(+)* control animals (progeny of *+/hT2* animals) were allowed to hatch on RNAi plates containing a bacterial feeding strain expressing L4440, an empty RNAi vector control. Pharyngeal pumping was determined at day 3 post hatching (Figure 11B). In agreement with previous findings (Dimitriadi et al, 2010), *smn-1(ok355)* animals display a significant reduction in pharyngeal pumping (44 ± 6) compared to *smn-1(+)* controls (217 ± 6) ($p = < 0.0001$). These findings illustrate that loss SMN-1 in *C. elegans* results in a 79.7% decrease in pharyngeal pumps. This established neuromuscular phenotype provides an ideal baseline to assess RNAi mediated knockdown of candidate autophagy modifier genes.

3.2 – Generation of RNAi Feeding Clones

3.2.1 – Construction of *atg-3* and *atg-4.2* RNAi feeding constructs

The Ahringer RNAi library covers 86% of the *C. elegans* genome (Kamath & Ahringer, 2003), excluded by this coverage are the autophagy genes *atg-3* and *atg-4.2*. To generate RNAi feeding clones for these genes, PCR was used (primer sequences shown in Table 6) to amplify genomic fragments incorporating the largest exon of each gene. The amplified fragments were sub-cloned into the L4440 feeding vector between two inverted T7 promoters (Kamath et al, 2003). The resulting plasmid constructs were transformed into the bacterial strain HT115(DE3). Restriction digests were used to confirm the constructs contained the correct sized genomic fragments (Figures 14-15), followed by verification via Sanger sequencing.

As expected, double digest of the L4440 *atg-3* construct (Figure 14) with *XhoI* and *HindIII* restriction endonucleases liberates the *atg-3* genomic fragment from the digested L4440 vector and displays two bands upon agarose gel electrophoresis – 522bp and 2790bp, respectively. Undigested L4440 *atg-3* does not display these bands and instead shows a strong band at approximately 2000bp corresponding to the supercoiled plasmid.

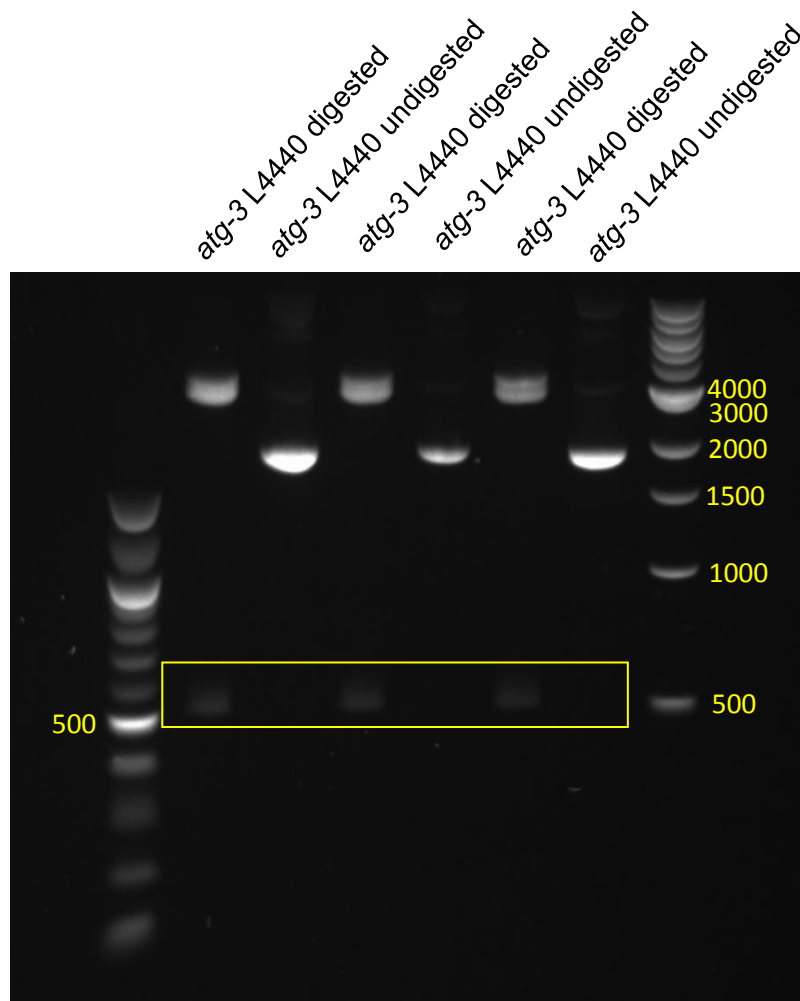


Figure 14. Restriction digest of the constructed L4440 *atg-3* plasmid liberates the *atg-3* genomic fragment from the L4440 plasmid. The *XhoI*/*HindIII* restriction digest was analysed with a 1% agarose gel electrophoresis. Double digestion of the L4440 *atg-3* plasmid construct produces a 522bp band corresponding to the *atg-3* genomic fragment and a digested plasmid band at 2790bp, compared to the undigested samples in which neither bands are present.

The same double digest of the L4440 *atg-4.2* construct (Figure 15) liberates the PCR fragment of the *atg-4.2* gene from the digested vector and displays two bands upon agarose gel electrophoresis – 596bp and 2790bp, respectively. The undigested samples do not display these bands, instead showing a single strong band at approximately 2000bp corresponding to plasmid supercoiling.

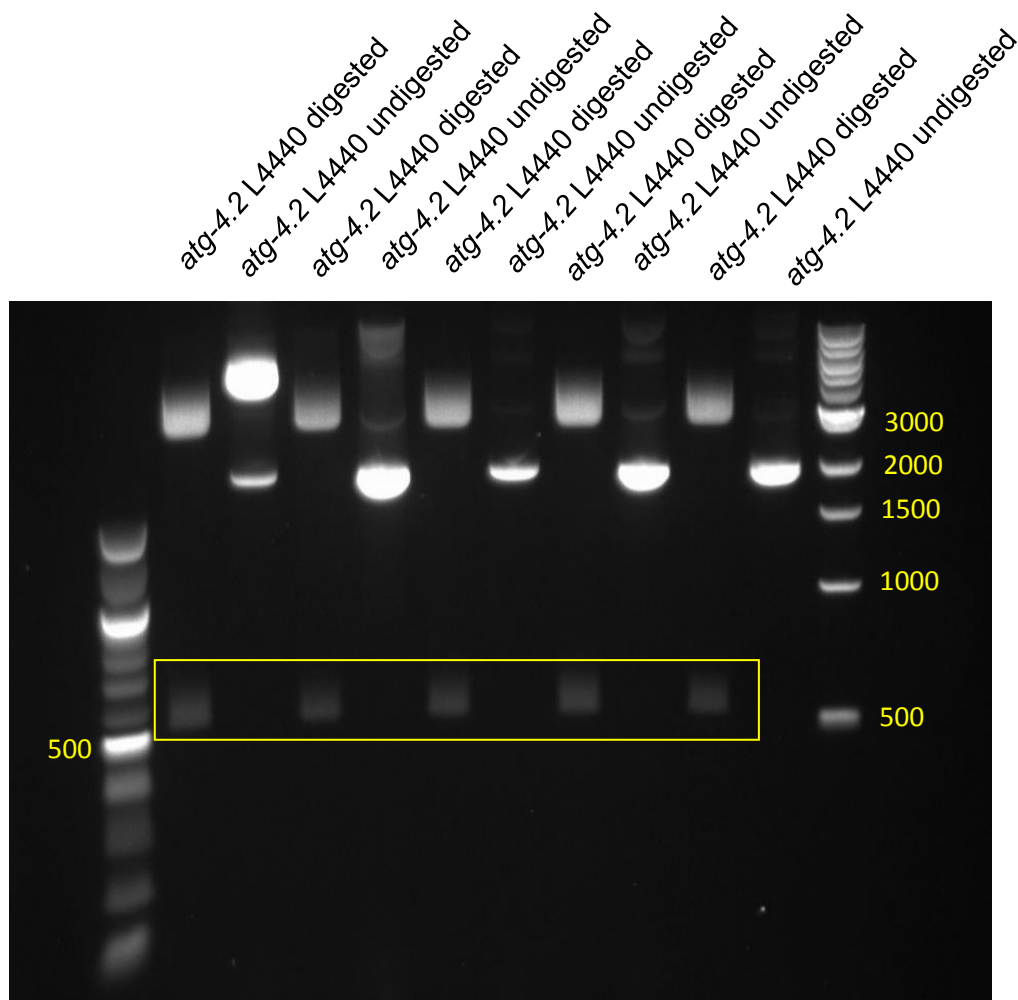


Figure 15. Restriction digest of the constructed L4440 *atg-4.2* plasmid liberates the *atg-4.2* genomic fragment from the L4440 plasmid. The *XhoI/HindIII* restriction digest was analysed with a 1% agarose gel electrophoresis. Double digestion of the L4440 *atg-4.2* plasmid construct produces a 596bp band corresponding to the *atg-4.2* genomic fragment and a digested plasmid band at 2790bp, compared to the undigested samples in which neither bands are present.

3.3 – Genetic Screen of Autophagy Orthologs in the *C. elegans* SMA Model

3.3.1 – RNAi mediated knockdown of several autophagy genes likely have no effect on SMN loss of function neuromuscular defects

To identify putative genes that modify SMN loss of function defects, a genetic screen of 22 *C. elegans* autophagy orthologs was undertaken to identify enhancers and suppressors of *smn-1(ok355)* neuromuscular defects. RNAi by feeding in *C. elegans* is known to be ineffective at targeting genes in certain tissues, including neurons, the vulva, sperm and the pharynx (Conte Jr., MacNeil, Walhout & Mello, 2017).

The transgene *uls72* express SID-1, a dsRNA channel protein, in motor neurons enabling the passive uptake of dsRNA and making RNAi by feeding more effective (Shih & Hunter, 2011). This transgene was crossed into the *+/hT2* and *smn-1/hT2* animals in order to facilitate effective neuronal RNAi (Calixto, Chelur, Topalidou, Chen & Chalfie, 2010). The animals used herein were derived from a *+/hT2; uls72* or *smn-1/hT2; uls72* genetic background.

Animals were allowed to hatch on RNAi plates with bacterial feeding strains expressing candidate gene dsRNA or control L4440 (empty RNAi vector). Pharyngeal pumping was used to assess animals at day 3 post-hatching and screen for genetic knockdowns that either suppress or enhance SMN loss of function defects in *smn-1(ok355)* animals. Assessment was made in second generation animals to ensure the RNAi effect was penetrant.

RNAi mediated knockdown of 19 out of 22 *C. elegans* autophagy orthologs had no significant effect on pharyngeal pumping in the *smn-1(ok355)* animals (Figures 16-21), these results are summarised below in Table 7. Interestingly, some gene knockdowns (*lgg-1*, *let-363*, *vps-34*, *unc-51* and *lgg-3*) significantly altered pharyngeal pumping in the *smn-1(+)* control animals. This is likely due to an SMN independent function of these genes or a non-specific effect of SID-1 expression.

Table 7. Nineteen autophagy genes had no significant effect on the SMN loss of function neuromuscular defects. Pharyngeal pumping rates of *smn-1(ok355)* and *smn-1(+)* control animals were determined by counting complete pharyngeal revolutions at 3 days post-hatching on bacterial feeding strains expressing dsRNA corresponding to candidate gene or L4440 (empty RNAi vector). Pharyngeal pumping rates are reported as the mean (\pm SEM) of all animals across all trials; percentage change was calculated as the percentage increase or decrease compared to control animals on L4440; Asterisks indicate significant difference determined using a Mann-Whitney *U* test, two tailed: **p* < 0.05, ***p* < 0.001, ****p* < 0.0001.

<i>C. elegans</i> gene	<i>smn-1(+)</i> L4440	<i>smn-1(+)</i> RNAi		<i>smn-1(ok355)</i> L4440	<i>smn-1(ok355)</i> RNAi	
	Pumps /min	Pumps /min	% change	Pumps /min	Pumps /min	% change
<i>lgg-1</i>	179 \pm 9	131 \pm 13 **	- 26.40%	48 \pm 7	41 \pm 6	- 14.58%
<i>bec-1</i>	164 \pm 10	145 \pm 14	- 11.59%	47 \pm 9	41 \pm 8	- 12.77%
<i>let-363</i>	180 \pm 12	138 \pm 16 *	- 23.33%	27 \pm 6	29 \pm 7	+ 7.41%
<i>vps-34</i>	180 \pm 12	124 \pm 13 **	- 31.11%	27 \pm 6	30 \pm 6	+ 11.11%
<i>unc-51</i>	167 \pm 12	106 \pm 15 **	- 36.53%	41 \pm 8	36 \pm 8	- 12.20%
<i>epg-1</i>	152 \pm 17	146 \pm 15	- 3.95%	37 \pm 7	27 \pm 6	- 27.03%
<i>vps-15</i>	152 \pm 17	140 \pm 14	- 7.89%	37 \pm 7	38 \pm 7	+ 2.70%
<i>atg-7</i>	145 \pm 12	143 \pm 12	- 1.38%	34 \pm 7	33 \pm 8	- 2.94%
<i>lgg-2</i>	171 \pm 9	130 \pm 12 *	- 23.98%	27 \pm 5	26 \pm 5	+ 3.85%
<i>atg-10</i>	171 \pm 9	166 \pm 10	- 2.92%	27 \pm 5	21 \pm 5	- 19.23%
<i>lgg-3</i>	171 \pm 15	208 \pm 12 *	+ 21.64%	38 \pm 10	42 \pm 9	+ 10.53%
<i>atg-5</i>	171 \pm 15	198 \pm 13	+ 15.79%	38 \pm 10	20 \pm 5	- 47.37%
<i>atg-4.1</i>	189 \pm 9	177 \pm 12	- 6.35%	43 \pm 6	31 \pm 7	- 27.91%
<i>atg-16.2</i>	180 \pm 9	171 \pm 13	- 5.00%	33 \pm 8	43 \pm 11	+ 30.30%
<i>ced-9</i>	180 \pm 9	150 \pm 16	- 16.67%	33 \pm 8	21 \pm 6	- 36.36%
<i>atg-9</i>	166 \pm 12	174 \pm 9	+ 4.82%	40 \pm 8	50 \pm 10	+ 25.00%
<i>atg-18</i>	166 \pm 12	142 \pm 16	- 14.46%	40 \pm 8	48 \pm 8	+ 20.00%
<i>atg-3</i>	158 \pm 12	172 \pm 12	+ 8.90%	40 \pm 8	24 \pm 6	- 35.00%
<i>atg-4.2</i>	158 \pm 12	160 \pm 12	+ 1.24%	40 \pm 8	33 \pm 7	- 17.50%

RNAi mediated knockdown of *lgg-1* (Figure 16A), *bec-1* (Figure 16B) and *atg-4.1* (Figure 16C) had no significant effect on SMN loss of function neuromuscular defects. Compared to *smn-1(ok355)* animals on L4440 (empty RNAi vector) control; knockdown of *lgg-1* reduced pumping by 14.58% (41 ± 6), *bec-1* reduced pumping by 12.77% (41 ± 8) and *atg-4.1* reduced pumping by 27.91% (31 ± 7).

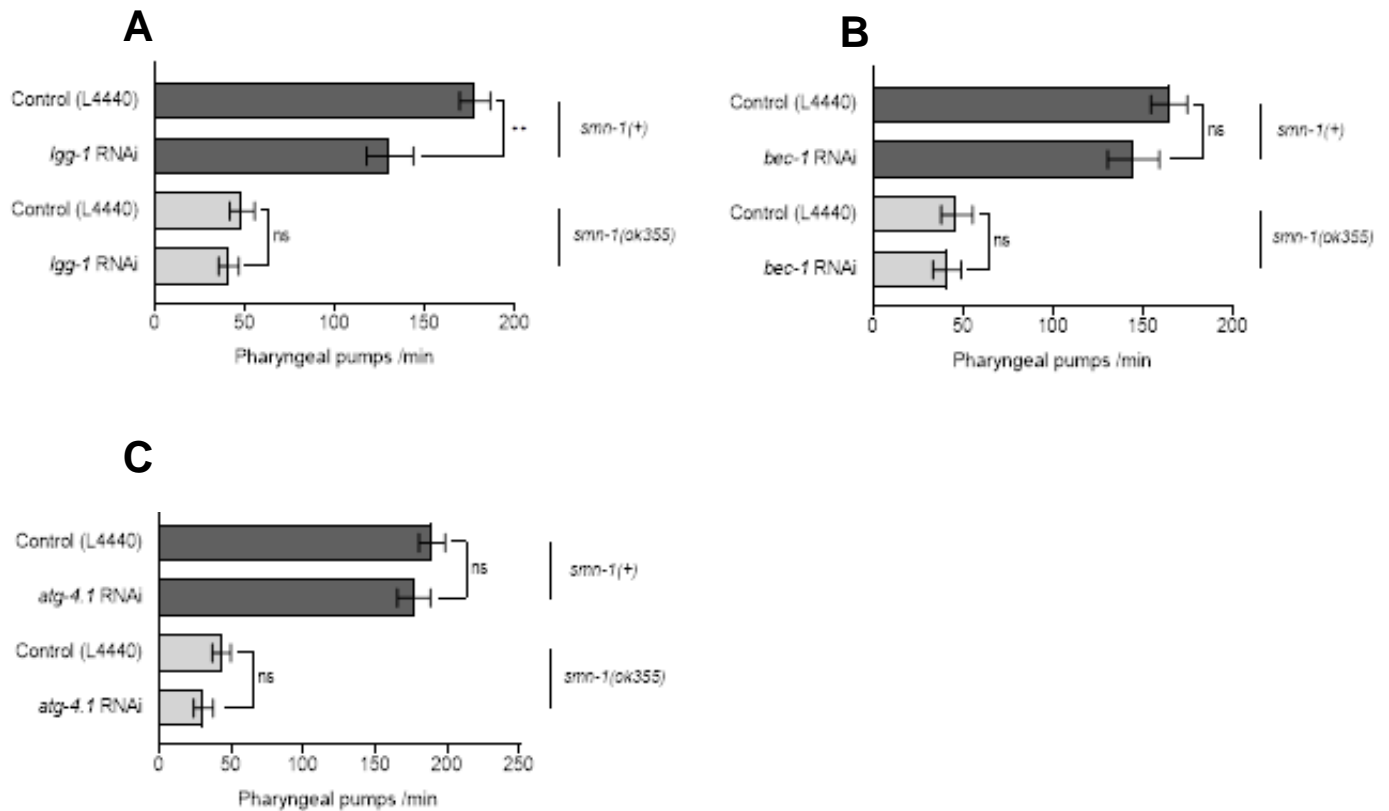


Figure 16. *C. elegans* autophagy orthologs *lgg-1*, *bec-1* and *atg-4.1* had no effect on the SMN loss of function neuromuscular defects. Pharyngeal pumping was determined in second generation *smn-1(ok355)* and *smn-1(+)* control animals at 3 days post-hatching on RNAi plates with bacterial feeding strains expressing dsRNA corresponding to *lgg-1*, *bec-1*, *atg-4.1* or L4440 (empty RNAi vector). (A) Knockdown of *lgg-1* had no significant effect on the pharyngeal pumping rates in *smn-1(ok355)* animals; (B) Knockdown of *bec-1* had no effect on the pharyngeal pumping rates in *smn-1(ok355)* animals; (C) Knockdown of *atg-4.1* had no significant effect on the pharyngeal pumping rates in *smn-1(ok355)* animals. Thirty animals were scored in total for each genotype across 3 independent trials. Error bars display \pm SEM; Asterisks indicate significant difference determined using a Mann-Whitney *U* test, two tailed: * $p < 0.05$, ** $p < 0.001$, *** $p < 0.0001$, ns - not significant.

RNAi mediated knockdown of *let-363* (Figure 17A) and *vps-34* (Figure 17B) had no significant effect on SMN loss of function neuromuscular defects. Compared to *smn-1(ok355)* animals on L4440 (empty RNAi vector); knockdown of *let-363* increased pumping by 7.41% (29 ± 7) and *vps-34* increased pumping by 11.11% (30 ± 6).

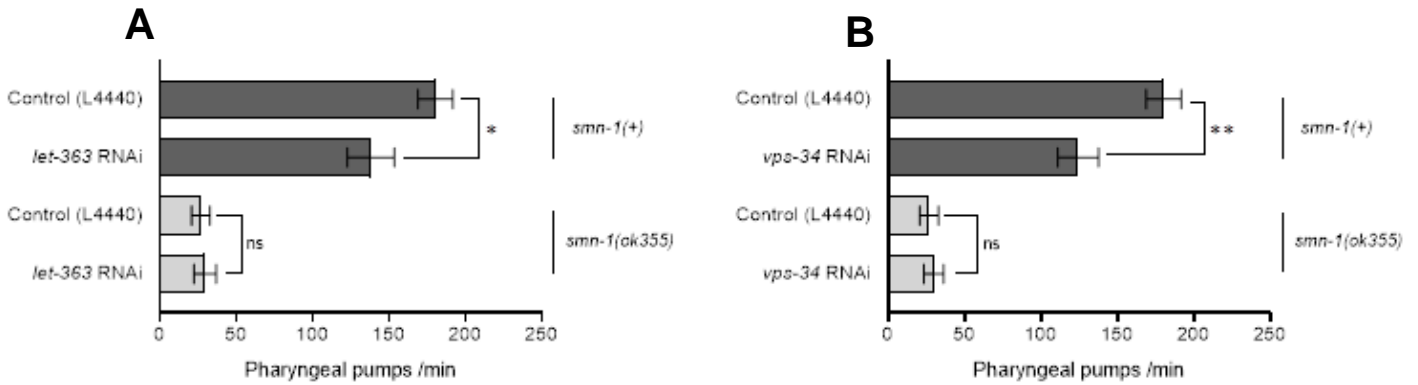


Figure 17. *C. elegans* autophagy orthologs *let-363* and *vps-34* had no effect on the SMN loss of function neuromuscular defects. Pharyngeal pumping was determined in second generation *smn-1(ok355)* and *smn-1(+)* control animals at 3 days post-hatching on RNAi plates with bacterial feeding strains expressing dsRNA corresponding to *let-363*, *vps-34* or L4440 (empty RNAi vector). (A) Knockdown of *let-363* had no significant effect on the pharyngeal pumping defects in *smn-1(ok355)* animals. (B) Knockdown of *vps-34* had no significant effect on the pharyngeal pumping defects in *smn-1(ok355)* animals. Thirty animals were scored for each gene knockdown or control across 3 independent trials. Error bars display \pm SEM; Asterisks indicate significant difference determined using a Mann-Whitney *U* test, two tailed: * $p < 0.05$, ** $p < 0.001$, *** $p < 0.0001$, *ns* - not significant.

RNAi mediated knockdown of *unc-51* (Figure 18A) and *atg-7* (Figure 18B) had no significant effect on SMN loss of function neuromuscular defects. Compared to *smn-1(ok355)* animals on L4440 (empty RNAi vector); knockdown of *unc-51* decreased pumping by 12.20% (36 ± 8) and *atg-7* reduced pumping by 2.94% (33 ± 8).

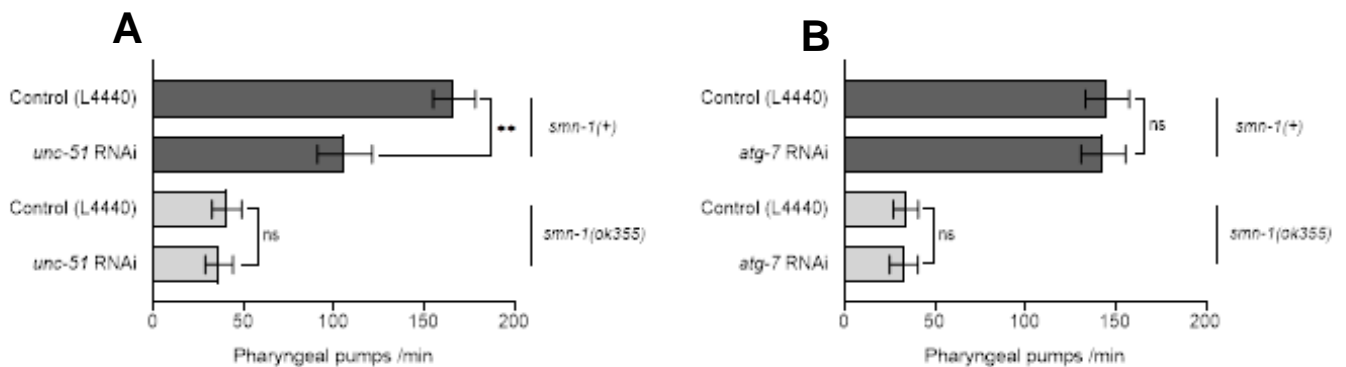


Figure 18. *C. elegans* autophagy orthologs *unc-51* and *atg-7* had no effect on the SMN loss of function neuromuscular defects. Pharyngeal pumping was determined in second generation *smn-1(ok355)* and *smn-1(+)* control animals at 3 days post-hatching on RNAi plates with bacterial feeding strains expressing dsRNA corresponding to *unc-51*, *atg-7* or L4440 (empty RNAi vector). (A) Knockdown of *unc-51* had no significant effect on the pharyngeal pumping defects in *smn-1(ok355)* animals. (B) Knockdown of *atg-7* had no significant effect on the pharyngeal pumping defects in *smn-1(ok355)* animals. Thirty animals were scored for each gene knockdown or control across 3 independent trials. Error bars display \pm SEM; Asterisks indicate significant difference determined using a Mann-Whitney *U* test, two tailed: * $p < 0.05$, ** $p < 0.001$, *** $p < 0.0001$, ns - not significant.

RNAi mediated knockdown of *epg-1* and *vps-15* (Figure 19A) had no significant effect on SMN loss of function neuromuscular defects. Compared to *smn-1(ok355)* animals on L4440 (empty RNAi vector); knockdown of *epg-1* decreased pumping by 27.03% (27 ± 6) whilst *vps-15* also increased pumping by 2.70% (38 ± 7). RNAi mediated knockdown of *lgg-2* and *atg-10* (Figure 19B) had no significant effect on SMN loss of function neuromuscular defects. Compared to *smn-1(ok355)* animals on L4440 (empty RNAi vector); knockdown of *lgg-2* increased pumping by 3.85% (26 ± 5) whereas *atg-10* reduced pumping by 19.23% (21 ± 5).

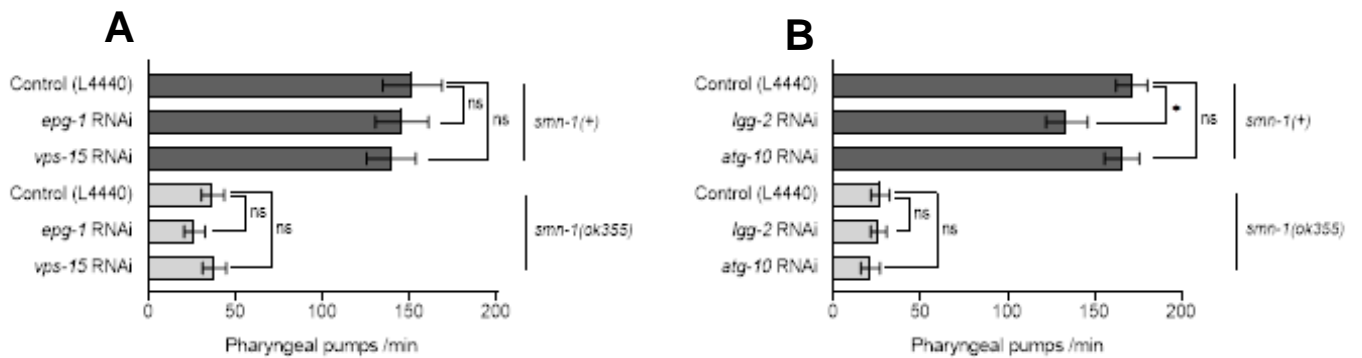


Figure 19. *C. elegans* autophagy orthologs *epg-1*, *vps-15*, *lgg-2* and *atg-10* had no effect on the SMN loss of function neuromuscular defects. Pharyngeal pumping was determined in second generation *smn-1(ok355)* and *smn-1(+)* control animals at 3 days post-hatching on RNAi plates with bacterial feeding strains expressing dsRNA corresponding to *epg-1*, *vps-15*, *lgg-2*, *atg-10* or L4440 (empty RNAi vector). (A) Knockdown of *epg-1* and *vps-15* had no significant effect on the pharyngeal pumping defects in *smn-1(ok355)* animals. (B) Knockdown of *lgg-2* and *atg-10* had no significant effect on the pharyngeal pumping defects in *smn-1(ok355)* animals. Fifty animals were scored for each gene knockdown or control across 3 independent trials. Error bars display \pm SEM; Asterisks indicate significant difference determined using a Mann-Whitney *U* test, two tailed: * $p < 0.05$, ** $p < 0.001$, *** $p < 0.0001$, *ns* - not significant.

RNAi mediated knockdown of *lgg-3* and *atg-5* (Figure 20A) had no significant effect on SMN loss of function neuromuscular defects. Compared to *smn-1(ok355)* animals on L4440 (empty RNAi vector); knockdown of *lgg-3* increased pumping by 10.53% (42 ± 9) whilst *atg-5* decreased pumping by 47.37% (20 ± 5). RNAi mediated knockdown of *atg-16.2* and *ced-9* (Figure 20B) had no significant effect on SMN loss of function neuromuscular defects. Compared to *smn-1(ok355)* animals on L4440 (empty RNAi vector); knockdown of *atg-16.2* increased pumping by 30.30% (43 ± 11) whereas *ced-9* reduced pumping by 36.36% (21 ± 6).

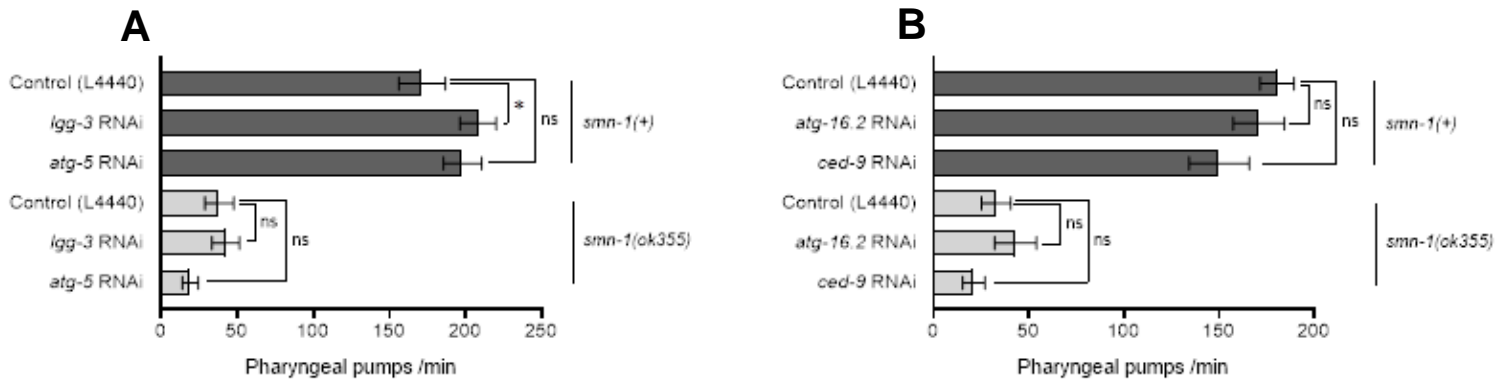


Figure 20. *C. elegans* autophagy orthologs *lgg-3*, *atg-5*, *atg-16.2* and *ced-9* had no effect on the SMN loss of function neuromuscular defects. Pharyngeal pumping was determined in second generation *smn-1(ok355)* and *smn-1(+)* control animals at 3 days post-hatching on RNAi plates with bacterial feeding strains expressing dsRNA corresponding to *lgg-3*, *atg-5*, *atg-16.2*, *ced-9* or L4440 (empty RNAi vector). (A) Knockdown of *lgg-3* and *atg-5* had no significant effect on the pharyngeal pumping defects in *smn-1(ok355)* animals. (B) Knockdown of *atg-16.2* and *ced-9* had no significant effect on the pharyngeal pumping defects in *smn-1(ok355)* animals. Thirty animals were scored for each gene knockdown or control across 3 independent trials. Error bars display \pm SEM; Asterisks indicate significant difference determined using a Mann-Whitney *U* test, two tailed: * $p < 0.05$, ** $p < 0.001$, *** $p < 0.0001$, ns - not significant.

RNAi mediated knockdown of *atg-9* and *atg-18* (Figure 21) had no significant effect on SMN loss of function neuromuscular defects. Compared to *smn-1(ok355)* animals on L4440 (empty RNAi vector); knockdown of *atg-9* increased pumping by 25.00% (50 ± 10) and *atg-18* also increased pumping by 20.00% (48 ± 8).

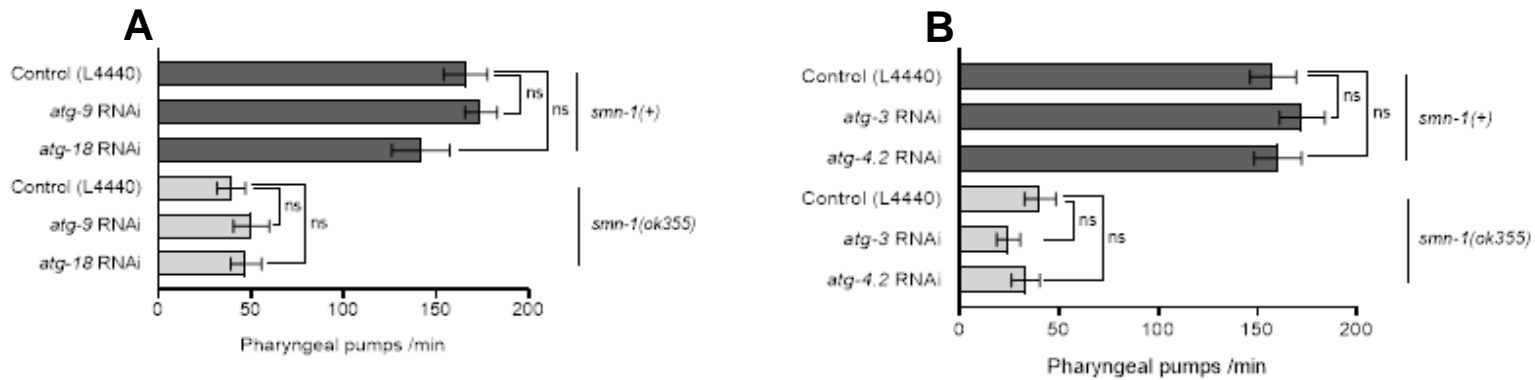


Figure 21. *C. elegans* autophagy orthologs *atg-9*, *atg-18*, *atg-3* and *atg-4.2* had no effect on the SMN loss of function neuromuscular defects. Pharyngeal pumping was determined in second generation *smn-1(ok355)* and *smn-1(+)* control animals at 3 days post-hatching on RNAi plates with bacterial feeding strains expressing dsRNA corresponding to *atg-9*, *atg-18* or L4440 (empty RNAi vector). (A) Knockdown of *atg-9* and *atg-18* had no significant effect on the pharyngeal pumping defects in *smn-1(ok355)* animals. (B) Knockdown of *atg-3* and *atg-4.2* had no significant effect on the pharyngeal pumping defects in *smn-1(ok355)* animals. Thirty animals were scored for each gene knockdown or control across 3 independent trials. Error bars display \pm SEM; Asterisks indicate significant difference determined using a Mann-Whitney *U* test, two tailed: * $p < 0.05$, ** $p < 0.001$, *** $p < 0.0001$, *ns* - not significant.

3.3.2 – Genetic screen identifies *epg-8*, *sqst-1* and *atg16.1* as putative modifiers of SMN loss of function neuromuscular defects

RNAi mediated knockdown of the *C. elegans* autophagy orthologs yielded three genes that act as putative modifiers of *smn-1(ok355)* neuromuscular defects. Of these three genes, *epg-8* was identified as a suppressor of SMN loss of function defects, whilst *sqst-1* and *atg-16.1* were identified as enhancers of SMN loss of function defects. Interestingly, we note that knockdown of these genes only affects pharyngeal pumping in *smn-1(ok355)* animals, indicating that these genes have an SMN specific function. These results are summarised below in Table 8.

Table 8. Three autophagy genes were identified as putative modifiers of SMN loss of function neuromuscular defects through an RNAi gene screen: *epg-8*, *sqst-1* and *atg-16.1*. Pharyngeal pumping rates of *smn-1(ok355)* and *smn-1(+)* control animals were determined by counting complete pharyngeal revolutions at 3 days post-hatching on bacterial feeding strains expressing dsRNA corresponding to candidate gene or L4440 (empty RNAi vector). Pharyngeal pumping rates are reported as the mean (\pm SEM) of all animals across all trials; percentage change was calculated as the percentage increase or decrease compared to control animals on L4440; Asterisks indicate significant difference determined using a Mann-Whitney *U* test, two tailed: **p* < 0.05, ***p* < 0.001, ****p* < 0.0001.

<i>C. elegans</i> gene	<i>smn-1(+)</i> L4440	<i>smn-1(+)</i> RNAi		<i>smn-1(ok355)</i> L4440	<i>smn-1(ok355)</i> RNAi	
	Pumps /min	Pumps /min	% change	Pumps /min	Pumps /min	% change
<i>epg-8</i>	160 \pm 9	168 \pm 10	+ 5.00%	32 \pm 5	52 \pm 7 *	+ 62.50%
<i>sqst-1</i>	167 \pm 12	179 \pm 12	+ 7.20%	41 \pm 8	13 \pm 4 **	- 68.30%
<i>atg-16.1</i>	189 \pm 9	181 \pm 11	- 4.20%	43 \pm 6	27 \pm 7 *	- 37.20%

The first gene identified as a putative modifier of SMN loss of function defects was *epg-8*, RNAi mediated knockdown of *epg-8* improved the *smn-1* loss of function neuromuscular defects in the *C. elegans* SMA model (Figure 22). Knockdown of *epg-8* significantly increased the number of pharyngeal pumps in *smn-1(ok355)* animals (52 \pm 7), compared to L4440 (empty RNAi vector) (32 \pm 5) by 62.5% (*p* = 0.0215). These results suggest that *epg-8* is likely acting as a suppressor of the SMN loss of function defects.

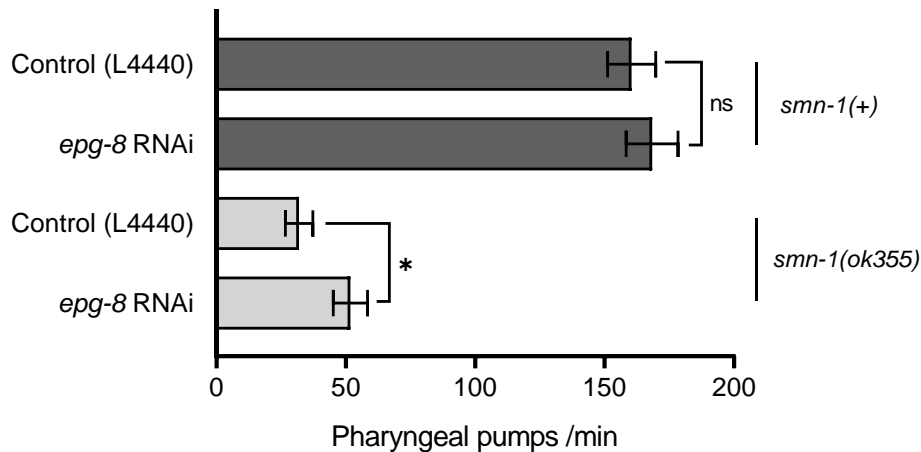


Figure 22. Knockdown of *C. elegans epg-8* suppresses pharyngeal pumping defects in *smn-1(ok355)* animals. Pharyngeal pumping rates of *smn-1(+)* and *smn-1(ok355)* animals were determined at 3 days post-hatching on bacterial feeding strains expressing dsRNA corresponding to *epg-8* or L4440 (empty RNAi vector). *epg-8* RNAi significantly increased pharyngeal pumping rates in *smn-1(ok355)* animals but had no significant effect in *+/smn-1(ok355)* animals. 50 animals were scored for each gene knockdown or control across 5 independent trials. Error bars display \pm SEM; Asterisks indicate significant difference determined using a Mann-Whitney *U* test, two tailed: * $p < 0.05$, ** $p < 0.001$, *** $p < 0.0001$, ns - not significant.

The next gene identified as a putative modifier of SMN loss of function defects was *sqst-1*. In contrast to *epg-8*, knockdown of *sqst-1* enhanced the *smn-1* loss of function defects in the *C. elegans* SMA model (Figure 23). In *smn-1(ok355)* animals, knockdown of *sqst-1* significantly decreased the number of pharyngeal pumps (13 ± 4) compared to animals on L4440 (empty RNAi vector) (41 ± 8), representing a 68.3% ($p = 0.0010$) decrease. These results suggest that *sqst-1* is acting as an enhancer of the SMN loss of function defects.

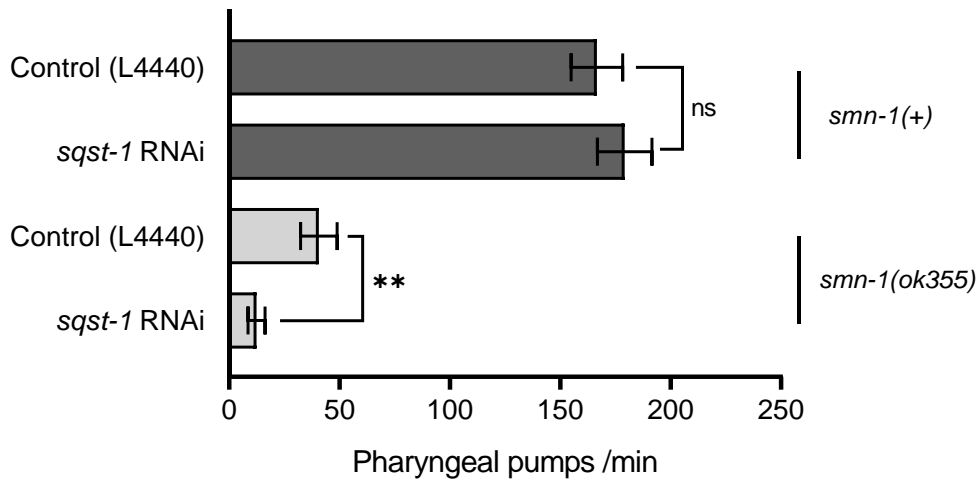


Figure 23. Knockdown of *C. elegans sqst-1* enhances pharyngeal pumping defects in *smn-1(ok355)* animals. Pharyngeal pumping rates of *smn-1(+)* and *smn-1(ok355)* animals were determined at 3 days post-hatching on bacterial feeding strains expressing dsRNA corresponding to *sqst-1* or L4440 (empty RNAi vector). *sqst-1* RNAi significantly decreased pharyngeal pumping rates in *smn-1(ok355)* animals but had no significant effect in *+/smn-1(ok355)* animals. Thirty animals were scored for each gene knockdown or control across 3 independent trials. Error bars display \pm SEM; Asterisks indicate significant difference determined using a Mann-Whitney *U* test, two tailed: * $p < 0.05$, ** $p < 0.001$, *** $p < 0.0001$, *ns* - not significant.

The last gene identified as a putative modifier of SMN loss of function defects was *atg-16.1*. Like *sqst-1*, knockdown of *atg-16.1* also exacerbated the *smn-1* loss of function defects in the *C. elegans* SMA model (Figure 24). Knockdown of *atg-16.1* through RNAi significantly decreased the pharyngeal pumps (27 ± 7) of *smn-1(ok355)* animals compared to the same animals on L4440 (empty RNAi vector) (43 ± 6), representing a 37.2% ($p = 0.0446$) decrease. These results suggest that *atg-16.1* is also acting as an enhancer of the SMN loss of function defects.

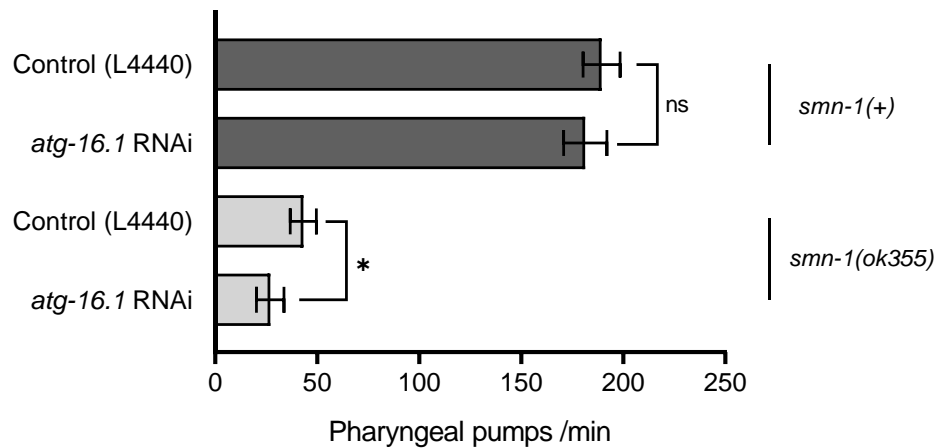


Figure 24. Knockdown of *C. elegans atg-16.1* enhances pharyngeal pumping defects in *smn-1(ok355)* animals. Pharyngeal pumping rates of *smn-1(+)* and *smn-1(ok355)* animals were determined at 3 days post-hatching on bacterial feeding strains expressing dsRNA corresponding to *atg-16.1* or L4440 (empty RNAi vector). *atg-16.1* RNAi significantly decreased pharyngeal pumping rates in *smn-1(ok355)* animals but had no significant effect in *+/smn-1(ok355)* animals. Thirty animals were scored for each gene knockdown or control across 3 independent trials. Error bars display \pm SEM; Asterisks indicate significant difference determined using a Mann-Whitney *U* test, two tailed: * $p < 0.05$, ** $p < 0.001$, *** $p < 0.0001$, ns - not significant.

4 Discussion

4.1 – Main Findings

Despite *SMN1* being discovered as the causative gene over a decade ago, it still remains unclear why depletion of the ubiquitously expressed SMN protein results in disease pathology specific toward motor neurons (Monani, 2005). Though the genetic components of SMA are very well characterised, the cellular and molecular pathways preceding disease pathogenesis remain elusive. It is well known that SMN depletion causes SMA but, due to a myriad of secondary functions (Table 2) it is still unknown which of these are pertinent to disease pathology. In the present study, we utilised the previously characterised invertebrate *C. elegans* SMA model (Briese et al, 2009), to perform an RNAi based genetic screen of 22 autophagy orthologs in order to identify putative genetic modifiers of SMN loss of function neuromuscular defects.

Using a pharyngeal pumping neuromuscular behavioural assay, we identified 3 autophagy genes that modified the pharyngeal pumping defects observed in the *C. elegans* SMA model. Identification of autophagy genes as putative modifiers of SMN loss of function neuromuscular defects indicates that autophagy may be perturbed in SMA, not only providing vital clues to the molecular mechanisms behind disease pathogenesis, but also identifying potential novel therapeutic targets.

4.2 – Autophagy is Disrupted in SMA

Several studies have shown that autophagy is disrupted in SMA using various *in vitro* and *in vivo* SMA models (Table 5). Garcera and colleagues (2013) first demonstrated that autophagy vesicles, namely autophagosomes, accumulated in mice motor neurons following *Smn* knockdown. In addition, Custer & Androphy (2014) demonstrated that autophagosomes accumulate in SMA motor neuron cell culture and SMA patient fibroblasts. Furthermore, Periyakruppiah and colleagues (2016) extended the initial findings by showing autophagic vesicles are elevated throughout development in a severe SMA mouse model and cultured *Smn* reduced mice motor neurons. Finally, an intermediate SMA mouse model was used to demonstrate that autophagosomes accumulated due to *Smn* decrease (Piras et al, 2017). The aforementioned studies note that the observed accumulation of autophagosomes could be the result of either increased autophagic activity, or a defect in the lysosomal fusion step which would prevent digestion of autophagosomes.

In order to determine whether autophagy was being upregulated or if flux was impaired, the studies utilised a variety of monitoring assays or pharmacological treatments with contradictory results (Table 5). Custer & Androphy (2014) and Periyakruppiah and colleagues (2016) made use of a p62/SQSTM1 monitoring assay to show that the levels of p62, a protein degraded by the action of autophagosome digestion (Larsen et al, 2010), are increased in SMN-depleted cells and an *in vitro* model of SMA suggested decreased autophagic flux. On the contrary, Garcera et al (2013) used Bafilomycin A1, a lysosomal inhibitor, to show the levels of autophagic markers were increased, indicating flux was unaffected in *Smn* reduced mice motor neurons. In addition, Piras et al (2017) used the p62/SQSTM1 monitoring assay to show that p62 levels were unchanged in the intermediate SMA mouse model. The same study used 3-methyladenine treatment, an autophagy inhibitor, demonstrating that autophagic markers were decreased and p62 levels were increased whilst motor neuron degeneration was delayed, and lifespan was increased. These results are consistent with the hypothesis that autophagy is upregulated in SMA, but autophagic flux is unaffected resulting in the accumulation of autophagic vesicles, however the topic remains a point of debate (Piras & Boido, 2018).

In addition, an independent study demonstrated that SMN protein levels are regulated by autophagy, and that lysosomal inhibition was sufficient to increase the levels of SMN (Rodriguez-Muela et al, 2017). The study first used coimmunoprecipitation assays to show that p62, an autophagy receptor and mediator of selective autophagy, interacts with SMN and that p62 levels are raised in SMA fibroblasts. These findings suggest that autophagic flux is disrupted, contradicting the previous studies. Furthermore, this study demonstrated that reduction of p62 increases the level of SMN, promoting motor neuron survival and increasing the lifespan of *Drosophila* and mouse SMA models. Rodriguez-Muela and colleagues (2017) suggest that p62 is upregulated in SMA resulting in degradation of SMN via selective autophagy.

Several studies published thus far have produced contradictory results regarding the precise nature of autophagic disruptions in SMA. Some of these studies show that autophagic flux is unaffected and autophagy disruptions are the result of overactive autophagy, whereas other studies show that autophagic flux is disrupted, although the role of this disruption is still heavily debated. Despite there are differences with these studies, there is strong consistent evidence that autophagic disruptions play a critical role in the disease pathology of SMA.

4.3 – Genes Identified as Modifiers of SMN Loss of Function Defects

The study presented here utilises the *C. elegans* SMA model and, through an RNAi based genetic screen identified three putative SMA modifier genes from the autophagy pathway (Figures 22-24). Using the pharyngeal pumping neuromuscular assay, *epg-8* (Figure 22) was identified as a suppressor of SMN loss of function neuromuscular defects whereas *sqst-1* and *atg-16.1* (Figures 23 and 24, respectively) were identified as enhancers of these defects.

The first of these putative modifiers, *epg-8*, suppressed the pharyngeal pumping defect in *smn-1(ok355)* animals when targeted by RNAi (Figure 22). This result suggests, for the first time to our knowledge, that *epg-8* may be involved in the pathology of SMA. *C. elegans* EPG-8 is orthologous to mammalian Atg14, a vital component of the vesicle nucleation that associates with the class III PI3K complex and enables initiation of the phagophore (Glick et al, 2010). Our results show that RNAi mediated knockdown of *epg-8* significantly increases pharyngeal pumping in *smn-1(ok355)* animals and thus suppresses SMN loss of function neuromuscular defects. This finding is consistent with the current hypothesis that autophagy is upregulated in SMA, since *epg-8* is required to direct proper autophagosome formation it is unsurprising that knockdown of this gene improved neuromuscular defects in the *C. elegans* SMA model.

We next identified *sqst-1*, the *C. elegans* ortholog of p62/SQSTM1, as a putative modifier of SMN loss of function defects. We found that *sqst-1* enhanced the pharyngeal pumping defect in *smn-1(ok355)* animals when silenced via RNAi (Figure 23). Like in mammalian systems, SQST-1 is an autophagosome receptor functions in binding the autophagosome and facilitating its fusion with the lysosome, SQST-1 thus has a pivotal and selective autophagy. Our results show that *sqst-1* knockdown exacerbates neuromuscular defects in the *C. elegans* SMA model, this contradicts the findings published by Rodriguez-Muela et al (2017) who demonstrate that reduction of p62 suppresses disease-associated SMA phenotypes.

This difference in findings may be due the nature of our RNAi experiments, SID-1 expression is known to decrease RNAi efficacy in non-neuronal tissues (Calixto et al, 2010), limiting RNAi effectiveness in these tissues which may explain our seemingly opposite results. Not only does the study conducted by Rodriguez-Muela and colleagues (2017) systemically target p62, using short hairpin RNA (shRNA) lentiviral transfection, but it was also conducted in *Drosophila* which may have other non-homologous interactions to consider. These findings highlight the need for further investigation into the precise role p62 plays in SMA disease pathology

Finally, we identified *atg-16.1* as another putative modifier of SMN loss of function defects in the *C. elegans* model. Like *sqst-1*, we found that knockdown of *atg-16.1* enhanced the pharyngeal pumping defects in *smn-1(ok355)* animals (Figure 24). ATG-16.1 is orthologous to mammalian Atg-16 and performs an equivalent function in phagophore expansion forming the mature autophagosome. As with *epg-8*, our results suggest for the first time that this protein may be involved in SMA disease pathology. Building on the hypothesis that autophagy disruption in SMA is due to autophagy upregulation; knockdown of *atg-16.1* would impair phagophore and inhibit autophagosome production, we would therefore expect that

knockdown of these gene should suppress SMA associated disease phenotypes rather than enhance them. In light of this, it is appealing to speculate that autophagy disruption in SMA occurs during the initial regulation steps rather than the downstream autophagosome maturation.

Taken together, these results indicate that the autophagic pathway holds promising potential for the discovery of novel therapeutic targets and treatment options although further studies are required to solidify our understanding of how autophagic disruptions are involved in SMA disease pathology. The main therapeutic approaches for SMA treatment currently revolve around increasing the levels of FL-SMN at the transcriptional level either by modifying *SMN2* splicing or using viral gene therapy to replace mutated *SMN1*. The possible therapeutic targets of the autophagic pathway would likely be non-SMN therapies but, to date only a handful of potential treatments do not target SMN directly and, therapeutics of this avenue have been explored in the clinical arena but have only enjoyed a modicum of success (Faravelli et al, 2015; Bowerman et al, 2017).

4.4 – Future Work

The preliminary data presented here suggests that the autophagic pathway genes *epg-8*, *sqst-1* and *atg-16.1* may have a potential role as modifiers of SMN loss of function neuromuscular defects in the *C. elegans* SMA model. Further study is required to determine the specificity of the putative genetic modifiers identified here and to characterise the full extent of autophagic disruptions in this model.

Firstly, to address the specificity of the putative genetic modifiers identified here, mutant alleles should be used to construct genetic double mutants. These double mutants will be assessed with the same pharyngeal pumping in order to confirm the initial RNAi data presented here. RNAi knockdown of genes in *C. elegans* via the feeding method is known to be effective in all tissues; with the exception of neurons, vulval tissue, sperm and the pharynx (Conte Jr., MacNeil, Walhout & Mello, 2017) where RNAi can be ineffective and result in only partial gene loss (Dimitriadi et al, 2010).

To assess the role autophagy plays in the *C. elegans* SMA model, the autophagic defects will require characterisation in *smn-1(ok355)* animals. To characterise these defects at a molecular level, a monitoring assay will first need to be established, several autophagy markers are available as reporter constructs in *C. elegans* (Papandreou & Tavernarakis, 2017). Among these reporters is the widely used GFP::LGG-1 fluorescent marker (orthologues to mammalian LC3) (Zhang et al, 2015), LGG-1 is a vital membrane coating protein present in every autophagosome. LGG-1 is normally present in the cytoplasm where it shows a diffuse expression pattern, when LGG-1 incorporated into the growing autophagosome structure, this expression pattern forms distinctive fluorescent puncta which can be monitored via fluorescent microscopy (Palmisiano & Melendez, 2016). In addition to the LGG-1 reporter, several other *C. elegans* autophagy orthologs can be expressed as fluorescent reporters; including BEC-1, ATG-4.1, ATG-9 and ATG-18 (Chen, Scarcelli & Legouis, 2017) which provide a wide range of methods to characterise autophagosome localisation in the *C. elegans* SMA model compared to control animals. Whilst several markers are available to monitor the localisation of autophagic bodies in *C. elegans*, they are not sufficient to discriminate between an upregulation in autophagy or impaired autophagic flux. Whilst fluorescent markers for p62 are

available, it is difficult to monitor them via fluorescent microscopy due to the rate of basal flux resulting in their degradation (Papandreou & Tavernarakis, 2017). As a result, a monitoring assay for p62 has not yet been described, instead autophagic flux can be determined in *C. elegans* using a combination of tandem fluorescent markers and lysosomal inhibitors (Kumsta, Chang, Schmalz & Hansen, 2017). The tandem GFP::mCherry::LGG-1 fluorescent construct is able to differentiate between autophagosomes and autolysosomes due to the different sensitivities of GFP and mCherry to acidic environments. Autophagosomes display GFP and mCherry puncta, however when the autophagosome fuses with the lysosome the GFP signal is quenched and only the mCherry puncta can be detected (Chen, Scarcelli & Legouis, 2017). This marker can be used to assess the number of autolysosomes present after treatment with inhibitors such as bafilomycin A1 to determine autophagic flux (Chang, Kumsta, Hellman, Adams & Hansen, 2017; Kumsta et al, 2017).

Using the aforementioned markers in the *C. elegans* SMA model will enable a characterisation of autophagy at a molecular level in the *smn-1(ok355)* animals compared to wild type animals. Once a characterisation of autophagy defects has been established, mutant alleles for *epg-8*, *sqst-1* and *atg-16.1* can be used to create genetic double mutants with *smn-1(ok355)* animals expressing reporter constructs. These double mutants can be used to assess whether putative genetic modifiers identified in this study ameliorate the autophagy defects we characterise.

Finally, the putative genetic modifiers identified in this study can be used to pinpoint specific protein complexes that are dysregulated in the *C. elegans* SMA model. Pharmacological challenges would be utilised to assess the effects of a series of autophagy activators or inhibitors on the *smn-1* neuromuscular defects. Animals would be treated with autophagy activators (e.g. spermidine, fluphenazine, resveratrol) or inhibitors (e.g. 3-methyladenine, wortmannin, bafilomycin) to determine their effects on pharyngeal pumping and the localisation of autophagic bodies (Galluzi, Pedro, Levine, Green & Kroemer, 2017). Each of the aforementioned compounds has a distinct biochemical target on autophagy and thus, any compound that impacts *smn-1* loss of function defects would indicate the disturbed autophagy networks (Galluzi et al, 2017).

4.5 – Conclusions

Considerable progress has been made into understanding how perturbations of the autophagic pathways may contribute to SMA pathology (Piras & Boido, 2018). During the last 5 years, a variety of *in vivo* and *in vitro* SMA models have been used to demonstrate that autophagosomes accumulate while flux remains unaffected, suggesting that accumulation of autophagic bodies is likely due to an upregulation of the pathway rather than a failure in their clearance (Garcera, et al, 2013; Custer & Androphy, 2014; Periyakaruppiyah et al, 2016; Piras et al, 2017). Furthermore, an independent study by Dimitriadi and colleagues (2016) identified that SMN depletion results in impaired endocytic trafficking, providing the first evidence endocytic pathways are disrupted in SMA. Building on this evidence, a subsequent study from the Wirth lab demonstrated that knockdown of NCALD ameliorated SMA disruptions by restoring endocytic function (Riessland et al, 2017).

The genetic screen presented in this study demonstrates that autophagy orthologs can act as putative modifier genes in the *C. elegans* SMA model by suppressing and enhancing the well characterised neuromuscular defects that arise due to deletion of the orthologous SMN-1

protein. We identified *epg-8* as a putative suppressor of SMN loss of function neuromuscular defects, *epg-8* is a vital positive regulator of the vesicle nucleation complex which serves to promote phagophore elongation upon autophagy induction. In line with the hypothesis that autophagy disruptions in SMA are due to upregulation, it is tempting to postulate that inhibition of *epg-8* may be an attractive therapeutic avenue for SMA although further study is required to determine its precise role in disease pathology.

In conclusion, the precise molecular mechanisms underlying SMA pathogenesis have yet to be elucidated however, impairment of the autophagic pathway is becoming an increasingly interesting avenue of SMA research and holds promise in identifying the molecular components of the disease pathology. Autophagy represents an exciting aspect of research, not only for its potential in revealing potential SMA treatment strategies, but also because impaired autophagy has been linked with other neurodegenerative disorders due to its role in clearing misfolded protein aggregates. Therefore, a deeper understanding of the roles autophagic pathways play in the pathology of SMA has potential in elucidating the pathologies behind other neurodegenerative disorders. The findings presented here in combination with results from other studies clearly demonstrate that autophagy is disrupted in several SMA models however, the exact role autophagy plays in the pathology of SMA remains under debate. Further research is required to determine the exact nature of this disruption before it can be translated toward patient benefits.

5 References

Ackermann B, Krober S, Torres-Benito L, et al. (2013) Plastin 3 ameliorates spinal muscular atrophy via delayed axon pruning and improves neuromuscular junction functionality. *Human Molecular Genetics*, 22, 1328–1347.

Ahmad, S., Wang, Y., Shaik, G. M., Burghes, A. H., & Gangwani, L. (2012). The zinc finger protein ZPR1 is a potential modifier of spinal muscular atrophy. *Human Molecular Genetics*, 21(12), 2745-2758.

Akten B, Kye MJ, Hao Le T, et al. (2014) Interaction of survival of motor neuron (SMN) and HuD proteins with mRNA cpg15 rescues motor neuron axonal deficits. *Proc Natl Acad Sci USA*, 8, 10337–10342.

Badadani, M. (2012). Autophagy Mechanism, Regulation, Functions and Disorders. *ISRN Cell Biology*, 2012, doi: 10.5402/2012/927064.

Battle, D. J., Kasim, M., Yong, J., Lotti, F., Lau, C. K., Mouaikel, J., et al. (2006). The SMN complex: an assembly machine for RNPs. *Cold Spring Harb Symp Quant Biol*, 71, 313-320. doi:10.1101/sqb.2006.71.001

Boda, B., Mas, C., Giudicelli, C., Nepote, V., Guimiot, F., Levacher, B., et al. (2004). Survival motor neuron SMN1 and SMN2 gene promoters: identical sequences and differential expression in neurons and non-neuronal cells. *European Journal of Human Genetics*, 12(9), 729-737.

Bowerman, M., Anderson, C. L., Beauvais, A., Boyd, P. P., Witke, W., & Kothary, R. (2007). SMN, profilin IIa and plastin 3: a link between the deregulation of actin dynamics and SMA pathogenesis. *Molecular and Cellular Neuroscience*, 42(1), 66-74.

- Bowerman, M., Becker, C.G., Yáñez-Muñoz, R.J., Ning, K., Wood, M.J.A., Gillingwater, T.H. et al. (2017). Therapeutic strategies for spinal muscular atrophy: SMN and beyond. *Disease Models & Mechanisms*, 10, 943-954.
- Boya, P., Reggiori, F. & Codogno, P. (2013). Emerging regulation and functions of autophagy. *Nature Cell Biology*, 15(7), 713-720.
- Brenner, S. (1974). The Genetics of *Caenorhabditis elegans*. *Genetics*, 77, 71-94.
- Briese, M. et al. (2009). Deletion of *smn-1*, the *Caenorhabditis elegans* ortholog of the spinal muscular atrophy gene, results in locomotor dysfunction and reduced lifespan. *Human Molecular Genetics*, 18(1), 97-104.
- Burghes, H.M. & Beattie, C.E. (2009). Spinal Muscular Atrophy: Why do low levels of SMN make motor neurons sick? *Nature Reviews Neuroscience*, 10(8), 597-609.
- Calixto, A., Chelur, D., Topalidou, I., Chen, X. & Chalfie, M. (2010). Enhanced neuronal RNAi in *C. elegans* using SID-1. *Nature Methods*, 7(7), 554-559.
- Cartegni, L. & Krainer, A.R. (2002). Disruption of an SF2/ASF-dependant exonic splicing enhancer in *SMN2* causes spinal muscular atrophy in the absence of *SMN1*. *Nature Genetics*, 30, 377-384.
- Chang, J.T., Kumsta, C., Hellman, A.B., Adams, L.M. & Hansen, M. (2017). Spatiotemporal regulation of autophagy during *Caenorhabditis elegans* aging. *eLife*, 6, doi: 10.7554/eLife.18459.
- Chen, Y., Scarcelli, V. & Legouis, R. (2017). Approaches for Studying Autophagy in *Caenorhabditis elegans*. *Cells*, 6(27), 1-19.
- Cherra, S.J. & Chu, C.T. (2008). Autophagy in neuroprotection and neurodegeneration: A question of balance. *Future Neurology*, 3(3), 309-323.
- Comely, L.H., Nijssen, J., Frost-Nylen, J. & Hedlund, E. (2016). Cross-disease comparison of amyotrophic lateral sclerosis and spinal muscular atrophy reveals conservation of selective vulnerability but differential neuromuscular junction pathology. *The Journal of Comparative Neurology*, 524(7), 1424-1442.
- Conte Jr, D., MacNeil, L.T., Walhout, A.J.M., Mello, C.C. (2017). RNA Interference in *Caenorhabditis elegans*. *Current Protocols in Molecular Biology*, 109, doi: 10.1002/0471142727.mb2603s109.
- Custer, S.K. & Androphy, E.J. (2014). Autophagy dysregulation in cell culture and animal models of spinal muscular atrophy. *Molecular and cellular Neuroscience*, 61, 133-140.
- D'Amico, A., Mercuri, E., Tiziano, F.D. & Bertini, E. (2011). Spinal muscular atrophy. *Orphanet Journal of Rare Diseases*, 6(71), doi: 10.1186/1750-1172-6-71.
- Deenen, J.C.W., Horlings, C.G.C., Verschuuren, J.M., Verbeek, A.L.M. & van Engelen, B. (2015). The Epidemiology of Neuromuscular Disorders: A Comprehensive Overview of the Literature. *Journal of Neuromuscular Diseases*, 2, 73-85.
- Dimitriadi, M., Derdowski, A., Kalloo, G., Maginnis, M.S., O'hern, P., Bliska, B., et al. (2016). Decreased function of survival motor neuron protein impairs endocytic pathways. *PNAS*, 113(30), doi: 10.1073.
- Dimitriadi, M., Sleight, J.N., Walker, A., Chang, H.C., Sen, A., Kalloo, G., et al. (2010). Conserved Genes Act as Modifiers of Invertebrate SMN Loss of Function Defects. *PLoS Genetics*, 6(10), doi: 10.1371.

- Fallini, C., Bassel, G.J. & Rossol, W. (2012). Spinal muscular atrophy: The role of SMN in axonal mRNA regulation. *Brain Research*, 1462, 81-92.
- Farrar, M.A. & Kiernan, M.C. (2015). The Genetics of Spinal Muscular Atrophy: Progress and Challenges. *Neurotherapeutics*, 12(2), 290-302.
- Galluzi, L., Pedro, J.M., Levine, B., Green, D.R. & Kroemer, G. (2017). Pharmacological modulation of autophagy: therapeutic potential and persisting obstacles. *Nature Reviews Drug Discovery*, 16, 487-511.
- Garcera, A., Bahí, N., Periyakarupiah, A., Arumagum, S. & Soler, R.M. (2013). Survival motor neuron protein reduction deregulates autophagy in spinal cord motoneurons *in vitro*. *Cell Death and Disease*, 4, doi: 10.1038/cddis.2013.209.
- Glick, D., Barth, S. & Macleod, K.F. (2010). Autophagy: cellular and molecular mechanisms. *Journal of Pathology*, 221(1), 3-12.
- Gubitz, A.K., Feng, W. & Dreyfuss, G. (2004). The SMN complex. *Experimental Cell Research*, 296(1), 51-56.
- Hosseini-barkooie S., Peters, M., Torres-Benito, L., Rastetter, R.H., Hupperich, K., Hoffmann, A. et al (2016). The Power of Human Protective Modifiers: PLS3 and CORO1C Unravel Impaired Endocytosis in Spinal Muscular Atrophy and Rescue SMA Phenotype. *The American Journal of Human Genetics*, 99, 647-665.
- Hosseini-barkooie, S., Schneider, S. & Wirth, B. (2017). Advances in understanding the role of disease-associated proteins in spinal muscular atrophy. *Expert Review of Proteomics*, doi: 10.1080/14789450.2017.1345631.
- Kaifer, K. A., Villalón, E., Osman, E. Y., Glascock, J. J., Arnold, L. L., Cornelison, D. D., & Lorson, C. L. (2017). Plastin-3 extends survival and reduces severity in mouse models of Spinal muscular atrophy. *JCI insight*, 2(5), e89970.
- Kamath, R.S. & Ahringer, J. (2003). Genome-wide RNAi screening in *Caenorhabditis elegans*. *Methods*, 30, 313-321.
- Kamath, R.S., Fraser, A.G., Dong, Y., Poulin, G., Durbin, R., Gotta, M. et al. (2003). Systematic functional analysis of the *Caenorhabditis elegans* genome using RNAi. *Nature*, 421, 231-237.
- Kamath, R.S., Martinez-Campos, M., Zipperlen, P., Fraser, A.G. & Ahringer, J. (2001). Effectiveness of specific RNA-mediated interference through ingested double stranded RNA in *Caenorhabditis elegans*. *Genome Biology*, 2(1), doi: 10.1186/gb-2000-2-1-research0002.
- Kashima, T., Rao, N., David, C.J. & Manley, J.L. (2007). hnRNP A1 functions with specificity in repression of *SMN2* exon 7 splicing. *Human Molecular Genetics*, 16(24), 3149-3159.
- Kaur, J. & Debnath, J. (2015). Autophagy at the crossroads of catabolism and anabolism. *Nature Reviews Molecular Cell Biology*, 16, 461-472.
- Kaushik, S. & Cuervo, A.M. (2012). Chaperone-mediated autophagy: a unique way to enter the lysosome world. *Trends in Cellular Biology*, 22(8), 407-417.
- Kiernan, M.C., Vucic, S., Cheah, B.C., Turner, M.R., Eisen, A., Hardiman, O. et al (2011). Amyotrophic lateral sclerosis. *The Lancet*, 377(9769), 942-955.

- Klionsky, D.J. & Emr, S.D. (2000). Autophagy as a Regulated Pathway of Cellular Degradation. *Science*, 290(5497), 1717-1721.
- Kolb, S.J. & Kissel, J.T. (2011). Spinal muscular atrophy: a timely review. *Archives of neurology*, 68(8), 979-984.
- Kolb, S.J. & Kissel, J.T. (2015). Spinal Muscular Atrophy. *Neurologic Clinics*, 33(4), 831-846.
- Kolb, S.J., Battle, D.J. & Dreyfuss, G. (2007). Molecular Functions of the SMN Complex. *Journal of Child Neurology*, 8, 990-994.
- Kumsta, C., Chang, J.T., Schmalz, J. & Hansen, M. (2017). Hormetic heat stress and HSF-1 induce autophagy to improve survival and proteostasis in *C. elegans*. *Nature communication*, 8, doi: 10.1038/ncomms14337.
- Kuo, C., Hansen, M. & Troemel, E. (2017). Autophagy and innate immunity: Insights from invertebrate model organisms. *Autophagy*, 14(2), 233-242.
- Larsen, K.B. et al (2010). A reporter cell system to monitor autophagy based on p62/SQSTM1. *Autophagy*, 6, 784-793.
- Le, T.T., Pham, L.T., Butchbach, M.E., Zhang, H.L., Monani, U.R., Coovert, D.D., et al. (2005). SMNDelta7, the major product of the centromeric survival motor neuron (SMN2) gene, extends survival in mice with spinal muscular atrophy and associates with full-length SMN. *Human Molecular Genetics*, 14(6), 845-857.
- Lefebvre, S., Burglen, L., Reboullet, S., Clermont, O., Burlet, P., Violette, L. et al. (1995). Identification and Characterisation of a Spinal Muscular Atrophy-Determining Gene. *Cell*, 80, 155-165.
- Levine, B. & Klionsky, D.J. (2004). Development by Self-Digestion: Molecular Mechanisms and Biological Functions of Autophagy. *Developmental Cell*, 6, 463-477.
- Levine, B. & Kroemer, G. (2009). Autophagy in the Pathogenesis of Disease. *Cell*, 132, 27-42.
- Levine, B., Mizushima, N. & Virgin, H.W. (2011). Autophagy in immunity and inflammation. *Nature*, 469(7330), 323-335.
- Li, W.W., Li, J. & Bao, J.K. (2012). Microautophagy: lesser-known self-eating. *Cellular and Molecular Life Sciences*, 69(7), 1125-1136.
- Little, D., Valori, C. F., Mutsaers, C. A., Bennett, E. J., Wyles, M., Sharrack, B., Ning, K. (2015). PTEN Depletion Decreases Disease Severity and Modestly Prolongs Survival in a Mouse Model of Spinal Muscular Atrophy. *Molecular Therapy*, 23(2), 270-277.
- Liu, W.J., Ye, L., Huang, W.F., Guo, L.G., Xu, Z.G., Wu, H.L. et al. (2016). P62 links the autophagy pathway and the ubiquitin-proteasome system upon ubiquitinated protein degradation. *Cellular and Molecular Biology Letters*, 21(29), doi: 10.1186/s11658-016-0031-z.
- Lodish, H.F., Berk, A., Kaiser, C., Kreiger, M., Scott, M.P., Bretscher, A. et al. (2008). *Molecular Cell Biology* (6th ed.). San Francisco: W.H. Freeman.
- Lorson, C.L., Hahnen, E., Androphy, E.J. & Wirth, B. (1999). A single nucleotide in the *SMN* gene regulates splicing and is responsible for spinal muscular atrophy. *PNAS*, 96(11), 6307-6311.
- Lotti, F., Imlach, W.L., Saieva, L., Beck, E.S., Hao, L.T., Li, D.K. et al. (2012). A SMN-Dependant U12 Splicing Event Essential for Motor circuit Function. *Cell*, 151(2), 440-454.

- Megalou, E.V. & Tavernarakis, N. (2009). Autophagy in *Caenorhabditis elegans*. *Biochimica et Biophysica Acta*, 1793, 1444-1451.
- Mehrpour, M., Esclatine, A., Beau, I. & Codogno, P. (2010). Overview of macroautophagy regulation in mammalian cells. *Cell Research*, 20, 748-762.
- Meléndez, A. & Levine, B. (2009). *Autophagy in C. elegans*. (WormBook ed.). The *C. elegans* Research Community, WormBook, doi: 10.1895/wormbook.1.147.1.
- Miguel-Aliaga, I., Culetto, E., Walker, D.S., Baylis, H.A., Sattelle, D.B. & Davies, K.E. (1999). The *Caenorhabditis elegans* orthologue of the human gene responsible for spinal muscular atrophy is a maternal product critical for germline maturation and embryonic viability. *Human Molecular Genetics*, 8, 2133-2143.
- Mis, M.S.C., Brajkovic, S., Frattini, E., Di Fonzo, A. & Corti, S. (2016). Autophagy in motor neuron disease: Key pathogenic mechanisms and therapeutic targets. *Molecular and Cellular Neuroscience*, 72, 84-90.
- Mizushima, N. & Komatsu, M. (2011). Autophagy: Renovation of Cells and Tissues. *Cell*, 147, 728-741.
- Mizushima, N. (2007). Autophagy: process and function. *Genes and Development*, 21, 2861-2873.
- Monani, U. & De Vivo, D.C. (2014). Neurodegeneration in spinal muscular atrophy: from disease phenotype and animal models to therapeutic strategies and beyond. *Future Neurology*, 9(1), 49-65.
- Monani, U.R. (2005). Spinal Muscular Atrophy: A Deficiency in a Ubiquitous Protein; a Motor Neuron-Specific Disease. *Neuron*, 48(6), 885-896.
- Monani, U.R., Lorson, C.L., Parsons, D.W., Prior, T.W., Androphy, E.J., Burghes, A.H.M. et al. (1999). A single nucleotide difference that alters splicing patterns distinguishes the SMA gene *SMN1* from the copy gene *SMN2*. *Human Molecular Genetics*, 8(7), 1177-1183.
- Moreau, K., Luo, S. & Rubinsztein, D.C. (2010). Cytoprotective roles for autophagy. *Current Opinion in Cell Biology*, 22(2), 206-211.
- Nah, J., Yuan, J. & Jung, Y. (2015). Autophagy in Neurodegenerative Diseases: From Mechanism to Therapeutic Approach. *Molecules and Cells*, 38(5), 381-389.
- Nixon, R.A. (2013). The role of autophagy in neurodegenerative disease. *Nature medicine*, 19(8), 983-997.
- Ohsumi, Y. (2014). Historical landmarks of autophagy research. *Cell Research*, 24, 9-23.
- Oprea, G.E., Kröber, S., McWhorter, M.L., Rossoll, W., Müller, S., Krawczak, M. et al. (2008). Plastin 3 is a protective modifier of autosomal recessive spinal muscular atrophy. *Science*, 320(5875), 524-527.
- Ottensen, E.W. (2017). ISS-N1 makes the first FDA-approved drug for spinal muscular atrophy. *Translational neuroscience*, 8(1), doi: 10.515.
- Otter, S., Grimmmler, M., Neuenkirchen, N., Chari, A., Sickmann, A. & Fischer, U. (2007). A Comprehensive Interaction Map of the Human Survival of Motor neuron (SMN) Complex. *Journal of Biological Chemistry*, 282(8), 5825-5833.

- Papandreou, M.E. & Tavernarakis, N. (2017). Monitoring Autophagic Responses in *Caenorhabditis elegans*. *Methods in Enzymology*, 588, 429-444.
- Parzych, K.R. & Klionsky, D.J. (2014). An Overview of Autophagy: Morphology, Mechanism and Regulation. *Antioxidants and Redox Signalling*, 20(3), 460-473.
- Pellizzoni, L., Yong, J. & Dreyfuss, G. (2002). Essential Role for the SMN Complex in the Specificity of snRNP Assembly. *Science*, 298, 1775-1779.
- Periyakaruppiyah, A., Fuente, S., Arumagum, S., Bahí, N., Garcera, A. & Soler, R.M. (2016). Autophagy modulators regulate survival motor neuron protein stability in motorneurons. *Experimental Neurology*, 283, 287-297.
- Piras, A., Schiaffino, L., Boido, M., Valsecchi, V., Guglielmo, M., De Amicis, E., et al. (2017). Inhibition of autophagy delays motoneuron degeneration and extends lifespan in a mouse model of spinal muscular atrophy. *Cell Death & Disease*, 8(12), 1-16.
- Piras, A., & Boido, M. (2018). Autophagy inhibition: a new therapeutic target in spinal muscular atrophy. *Neural Regen Res*, 13(5), 813-814. doi:10.4103/1673-5374.232473
- Renvoise, B., Khoobarry, K., Gendron, M. C., Cibert, C., Viollet, L., & Lefebvre, S. (2006). Distinct domains of the spinal muscular atrophy protein SMN are required for targeting to Cajal bodies in mammalian cells. *J Cell Sci*, 119(Pt 4), 680-692. doi:10.1242/jcs.02782
- Reggiori, F. & Klionsky, D.J. (2002). Autophagy in the Eukaryotic Cell. *Eukaryotic Cell*, 1(1), 11-21.
- Riddle, D.L., Blumenthal, T., Meyer, B.J. & Priess, J.R. (1977). *C. elegans II*. (2nd ed.). New York: Cold Spring Harbor Laboratory Press.
- Riddle, D.L., Blumenthal, T., Meyer, B.J. & Priess, J.R. (1997). *C. elegans II* (2nd ed.). New York: Cold Spring Harbor Laboratory Press.
- Riessland, M., Kaczmarek, A., Schneider, S., Swoboda, K.J., Löhr, H., Bradler, C. et al (2017). Neurocalcin Delta Suppression Protects against Spinal Muscular Atrophy in Humans and across Species by Restoring Impaired Endocytosis. *American Journal of Human genetics*, 100(2), 297-315.
- Rodriguez-Meula, N. et al. (2017). Blocking p62-dependant SMN degradation ameliorates spinal muscular atrophy disease phenotypes. *Journal of Clinical Investigation*, 128(7), 3008-3021
- Rossol, W., Jablonka, S., Andreassi, C., Kröning, A.K., Karle, K., Umrao, R. et al (2003). Smn, the spinal muscular atrophy-determining gene product, modulates axon growth and localization of β -actin mRNA in growth cones of motor neurons. *The Journal of Cell Biology*, 163(4), 801-812.
- Rusten, T.E. & Stenmark, H. (2010). P62, an autophagy hero or culprit? *Nature cell biology*, 12(3), 207-209.
- Son, H. W., & Yokota, T. (2018). Recent Advances and Clinical Applications of Exon Inclusion for Spinal Muscular Atrophy. *Methods Mol Biol*, 1828, 57-68. doi:10.1007/978-1-4939-8651_4_3
- Singh, N.N. & Singh, R.N. (2011). Alternative splicing in spinal muscular atrophy underscores the role of an intron definition model. *RNA Biology*, 8(4), 600-606.
- Sulston, J.E. & Horvitz, H.R. (1977). Post-embryonic cell lineages of the nematode *Caenorhabditis elegans*. *Developmental Biology*, 56, 110-156,
- Sulston, J.E., Schierenberg, E., White, J.G. & Thomson, J.N. (1983). The embryonic cell lineage of the nematode *Caenorhabditis elegans*. *Developmental Biology*, 100, 64-119.

- Timmons, L. & Fire, A. (1998). Specific interference by ingested dsRNA. *Nature*, 395, 854.
- Timmons, L., Court, D.L. & Fire, A. (2001). Ingestion of bacterially expressed dsRNAs can produce specific and potent genetic interference in *Caenorhabditis elegans*. *Gene*, 263, 103-112.
- Tiryaki, E. & Horak, H.A. (2014). ALS and other motor neuron diseases. *Continuum*, 20(5), 1158-1207.
- Trojanowski, N.F., Raizen, D.M. & Fang-Yen, C. (2016). Pharyngeal pumping in *Caenorhabditis elegans* depends on tonic and phasic signalling from the nervous system. *Scientific Reports*, 6, article number: 22940.
- Verhaart, I.E.C., Robertson, A., Wilson, I.J., Aartsma-Rus, A., Cameron, S., Jones, C.C. et al (2017). Prevalence, incidence and carrier frequency of 5q-linked spinal muscular atrophy – a literature review. *Orphanet Journal of Rare Diseases*, 12(124), doi: 10.1186/s13023-017-0671-8.
- Wang, D., Peng, Z., Ren, G. & Wang, G. (2015). The different roles of selective autophagic protein degradation in mammalian cells. *Oncotarget*, 6(35), 37098-37116.
- White, J.G., Southgate, E., Thomson, J.N. & Brenner, S. (1986). The structure of the nervous system of *C. elegans*. *Philosophical Transactions of the Royal Society*, 314, 1-340.
- Wirth, B., Brichta, L., Schrank, B., Lochmüller, H., Blick, S., Baasner, A. et al. (2006). Mildly affected patients with spinal muscular atrophy are partially protected by an increased *SMN2* copy number. *Human Genetics*, 119(4), 422-428.
- Wood, M.J.A., Talbot, K., & Bowerman, M. (2017). Spinal muscular atrophy: antisense oligonucleotide therapy opens the door to an integrated therapeutic landscape. *Human Molecular Genetics*, 26(2), 151-159.
- Yang, D.J., Zhu, L., Ren, J., Zhu, H. & Xu, J. (2015). Dysfunction of autophagy as the pathological mechanism of motor neuron disease based on a patient-specific disease model. *Neuroscience Bulletin*, 31(4), 445-451.
- Zarei, S., Carr, K., Reiley, L., Diaz, K., Guerra, O., Altamirano, P.F. et al. (2015). A comprehensive review of amyotrophic lateral sclerosis. *Surgical Neurology International*, 6(171), doi: 10.4103/2152-7806.169561.
- Zhang, Y., Chang, J.T., Gua, B., Hansen, M., Jia, K., Kovács, A.L. et al (2015). Guidelines for monitoring autophagy in *Caenorhabditis elegans*. *Autophagy*, 11(1), 9-27.